Analytical Computation of the Sensitivity Coefficients in Hybrid AC/DC Networks

Willem Lambrichts, Mario Paolone
Distributed Electrical Systems Laboratory, EPFL, Switzerland
willem.lambrichts@epfl.ch, mario.paolone@epfl.ch

***Abstract*—In this paper, we present a model for the analytical computation of the power flow sensitivity coefficients (SCs) for hybrid AC/DC networks. The SCs are defined as the partial derivates of the nodal voltages with respect to the active and reactive power injections and are used in the literature to model the grid constraints in a linear way (e.g. in real-time grid-aware control applications). The proposed method is inspired by an existing SC computation process proposed for AC networks and here suitably extended to include both the DC grid and the relevant AC/DC Interfacing Converters (ICs). The ICs can operate under different control modes i.e. voltage or power. Additionally, the model can compute the SCs for three-phase networks subjected to unbalanced loading conditions. The proposed method is numerically validated on a 26-node hybrid AC/DC microgrid and on a multiterminal HVDC network that links two asynchronous AC transmission grids. Furthermore, we provide a formal proof regarding the uniqueness of the proposed SCs computational model for hybrid AC/DC networks.**

***Index Terms*—Sensitivity coefficients, Hybrid AC/DC networks, HVDC, Optimal power flow, Unbalanced networks, Microgrids.**

I. Introduction

Hybrid AC/DC microgrids and multiterminal high voltage AC/DC grids are promising solutions for future power grids expected to host a large share of renewable sources. Integrating AC and DC networks has several advantages. 1) An increased overall efficiency of the system, because DC sources and loads are directly connected in the DC grid and thus fewer power conversion sources are required [1] 2) A lower infrastructure investment cost because of the material savings from cables and transformers. 3) A more flexible grid control that is mainly driven by the controllability of the AC/DC Interfacing Converters (ICs) [1], [2].

Real-time control is critical for the secure and optimal operation of hybrid AC/DC networks that are typically characterised by fast dynamics, caused by the ICs and the connected Distributed Energy Resources (DERs). One of the main blocks of any grid-aware real-time control is the Optimal Power Flow (OPF), which aims at computing the optimal setpoints of the controllable DERs in both the AC and DC grid and the optimal ICs' setpoints in order to minimize a certain objective [3]. Depending on the IC's operating mode, these setpoints can be powers (active or reactive) or voltages (AC or DC).

The OPF requires an accurate model of the hybrid network to formulate the grid constraints. Typically, this is defined by the power flow (PF) model. The PF equations for the AC network, DC network and ICs are non-linear and non-convex and, therefore, imply computational complexity to determine the global minimum.

To increase the tractability of the optimisation problem, these constraints are typically linearized or convexified using relaxation techniques [4]–[8]. This work focuses on the former approach where the power flow equations are linearized using the well-known Sensitivity Coefficients (SCs) concept. SCs are formally defined as the partial derivatives of the controlled variables (e.g. nodal voltages or branch currents) with respect to the controllable variables (e.g. power injections). Therefore, having an efficient computation method for the SCs is crucial for fast real-time control applications.

Traditionally, the SCs are computed relying on the inversion of the Jacobian matrix of the solved unified power flow problem. This method, however, has several major drawbacks. 1) It requires solving the full unified load flow of the AC/DC network to obtain the Jacobian matrix. Reference [9] shows that keeping the Jacobian matrix constant introduces significant errors, and would thus have to be recomputed frequently. 2) The Jacobian matrix does not allow to retrieve the SCs of nodes where the voltage is regulated, such as *PV nodes* in the AC system and *V-nodes* in the DC system. 3) The method always computes the full sensitivity matrix. This is a disadvantage in time-critical control applications where the full knowledge of the sensitivity matrix is not required, but only the SCs of certain controllable nodes.

Therefore, in this work, we present a method for the computation of the SCs (voltage and current) for balanced and unbalanced three-phase hybrid AC/DC networks that tackles all three of these above-listed problems. The method accounts for the different operation modes of the ICs, does not depend on the load flow Jacobian matrix and relies only on the network's admittance matrix and the state of the grid.

The paper is structured as follows: In Section II, the state-of-the-art on the SC computation techniques is reviewed. Section III briefly presents the unified PF model of the hybrid AC/DC network that is used in this work and introduces the nomenclature that is used throughout the paper. Section IV introduces the proposed analytical model that allows for the efficient computation of the voltage SCs in hybrid AC/DC networks. Furthermore, the computation of other SCs, such as the branch currents is discussed. In Section V, the proposed model is numerically validated on a hybrid AC/DC microgrid and an HVDC multiterminal transmission system.

The project has received funding from the European Unions Horizon 2020 Research & Innovation Programme under grant agreement No. 957788.

II. State-of-the-Art Review

The literature has presented several methods that allow for an efficient computation of the SCs. Most of the works, however, are only applicable to AC networks and are still based on the knowledge of the power flow Jacobian. Reference [10] proposes a method to compute the voltage SC without the need for the power flow Jacobian matrix, however, the method is only applicable to radial networks and does not account for the presence of branches shunt elements. In [11], a closed-form expression based on a first-order Taylor expansion is presented. The work also presents the second and third-order Taylor series expansions to improve the accuracy. In [12], a linear approximation of the balanced power flow solution is presented together with a sufficient condition for the existence of a solution. Both PQ and voltage-controlled (PV) are considered. Reference [9] proposes a closed-form method based on the Gauss-Seidel approximation and the Z-bus impedance matrix to express the SCs as explicit functions. References [13], [14] are also based on the impedance matrix. All these methods, however, still rely on the inversion of the PF Jacobian. In the application of hybrid AC/DC networks, reference [15] proposes a linear approximation where the square of the DC voltage is used as a controllable variable. The ICs' models are approximated using a first-order Taylor expansion.

The authors of [16], [17] developed a state-dependent linear model that allows for an efficient computation of the (AC network's) SCs, with a guaranteed uniqueness of the solution. Reference [18] extends this method to account for generic multiphase unbalanced networks with PQ and PV nodes and enables voltage-dependent nodal power injection models. This methodology only requires knowledge of the state of the grid and its admittance matrix. Reference [19] uses this method to express the linear grid constraints for an OPF problem. The authors show that when the SCs are updated dynamically, the convergence speed and accuracy are compatible with real-time control requirements.

In this work, we leverage the concept presented in [16], [17], to develop a computational model for the SCs in hybrid AC/DC networks with multiple ICs. The main challenge lies in the derivation of an accurate SC model that includes the AC network, DC network and the ICs that obey different control modes depending on their operation mode.

In view of the above, the main contribution of this work is the analytical SC computational model for hybrid AC/DC networks that guarantees the uniqueness of the SCs. The model accounts for all types of nodes in the AC and DC grid and for the different operating conditions of the ICs. The proposed model can be used for networks under unbalanced conditions and allows for intentionally negative sequence power injection. Furthermore, the model allows for multiple (AC) slack nodes, includes the filters and losses of the ICs and is applicable to both distributions and transmission systems.

III. Unified Power Flow Model for Hybrid AC/DC Networks

The proposed model for the computation of the voltage SC is derived using the unified PF model for hybrid AC/DC networks presented in the author's previous work [20]. The PF model includes the AC network, DC network and the ICs that can operate in different operating modes (voltage or power control). Compared to other works presented in the literature, the proposed method allows to consider multiple ICs to regulate the DC voltage [1].

We consider a generic hybrid AC/DC grid shown in Figure 1. The grid consists of $i \in \mathcal{N}$ AC nodes, $j \in \mathcal{M}$ DC nodes and the pair $(l,k) \in \mathcal{L}$ is a couple of AC/DC converter nodes. We assume that $l \in \mathcal{N}$ and $k \in \mathcal{M}$.

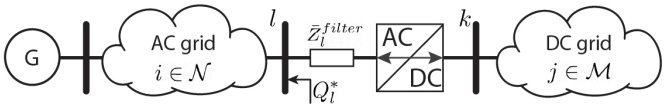

Fig. 1: The generic hybrid AC/DC network. Only one AC/DC converter is considered for simplicity.

The **AC system** is modelled using the traditional power system theory and consists of three types of nodes: a *Slack* node ($\mathcal{N}_{slack}$), *PQ* nodes ($\mathcal{N}_{PQ}$) and *PV* nodes ($\mathcal{N}_{PV}$). Furthermore, we assume that the zero-injection nodes can be modelled as *PQ* nodes. The AC network is described by its compound three-phase nodal admittance matrix $\overline{\mathbf{Y}}^{ac}$ that describes the relation between the phase-to-ground nodal voltages $\overline{\mathbf{E}}^{ac}$ and the nodal current injections $\bar{\mathbf{I}}^{ac}$: $\bar{\mathbf{I}}^{ac} = \overline{\mathbf{Y}}^{ac}\overline{\mathbf{E}}^{ac}$. The admittance matrix is constructed using the line impedances that are represented using the standard three-phase Π-equivalent model, see Figure 2. $\overline{Y}_{(i,n),L}$ is the longitudinal admittance between nodes i and n, and $\overline{Y}_{(i,n),T_i}$ and $\overline{Y}_{(i,n),T_n}$ are the shunt elements in node i and n. The compound admittance matrix is assumed to be known.

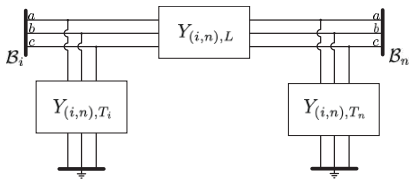

Fig. 2: The generic three-phase Π-equivalent branch model.

The **DC system** is modelled identically to the AC network using the classic AC theory where the electrical quantities are strictly real values: the reactive power $Q = 0$, the line impedance $\overline{Z} = R$ and the shunts are nil. Two types of controllable nodes are introduced: constant power nodes ($\mathcal{M}_{\mathcal{P}}$) and constant voltage nodes ($\mathcal{M}_{\mathcal{V}}$). The DC network is described by its compound admittance matrix. Therefore, $\mathbf{I}^{dc} = \mathbf{Y}^{dc}\mathbf{E}^{dc}$, where $\mathbf{E}^{dc}$ is the phase-to-ground nodal DC voltage vector, $\mathbf{I}^{dc}$ the nodal DC current injections and $\mathbf{Y}^{dc}$ the compound admittance matrix, which is again assumed to be known.

The **interfacing converters**, typically operated as Voltage Source Converters (VSCs), interface the AC and the DC

[1] It is worth noting that the presence of multiple voltage-controlled ICs results in an increased systems redundancy, improves the flexibility of the control and, generally, results in more realistic grid architectures [21].

system in one or more nodes (i.e., $|\mathcal{L}| \geq 1$)[2].

The control scheme allows the VSCs to operate in different modes and control different electrical quantities [22]. Usually, the control pairs are the active and reactive power injection: $P_{ac} - Q_{ac}$, or the DC voltage and the reactive power: $V_{dc} - Q_{ac}$. The VSCs use a phase-locked loop (PLL) -based control scheme to synchronise to the grid. During unbalanced loading conditions, the PLL typically synchronises to the positive sequence components to only inject positive sequence power, i.e., the homopolar and negative sequence components of the injected power are zero. In specific cases, the ICs can also intentionally inject negative sequence power to reduce the unbalanced loading conditions.

In conclusion, the set of AC and DC nodes is described as:

$$\mathcal{N} = \mathcal{N}_{slack} \cup \mathcal{N}_{PQ} \cup \mathcal{N}_{PV} \cup \mathcal{L}_{l,PQ} \cup \mathcal{L}_{l,V_{dc}Q},$$
$$\mathcal{M} = \mathcal{M}_{P_{dc}} \cup \mathcal{M}_{V_{dc}} \cup \mathcal{L}_{k,PQ} \cup \mathcal{L}_{k,V_{dc}Q},$$

and the different nodes in the hybrid AC/DC network are summarised in Table I. The nomenclature and indices of the node types of Table I are consistently used throughout this paper.

TABLE I: Different types of nodes in hybrid AC/DC networks and their known and unknown variables.

Bus Type	IC ctrl.	Known var.	Unknown var.	Index
AC slack		$\lvert E_{ac}\rvert$, $\angle E_{ac}$	P_{ac},Q_{ac}	$s \in \mathcal{N}_{slack}$
P_{ac}, Q_{ac}		P_{ac},Q_{ac}	$\lvert E_{ac}\rvert$, $\angle E_{ac}$	$i \in \mathcal{N}_{PQ}$
P_{ac}, $\lvert V_{ac}\rvert$		P_{ac},$\lvert V_{ac}\rvert$	Q_{ac}, $\angle E_{ac}$	$i \in \mathcal{N}_{PV}$
IC_{ac}	P - Q V_{dc} - Q	P_{ac} Q_{ac} Q_{ac}	$\lvert E_{ac}\rvert$, $\angle E_{ac}$ P_{ac}, $\lvert E_{ac}\rvert$, $\angle E_{ac}$	$l \in \mathcal{L}_{PQ}$ $l \in \mathcal{L}_{V_{dc}Q}$
IC_{dc}	P - Q V_{dc} - Q	P_{dc} E_{dc}	E_{dc} P_{dc}	$k \in \mathcal{L}_{PQ}$ $k \in \mathcal{L}_{V_{dc}Q}$
P_{dc}		P_{dc}	E_{dc}	$j \in \mathcal{M}_P$
E_{dc}		E_{dc}	P_{dc}	$j \in \mathcal{M}_V$

It is worth noticing that the DC grid doesn't have a 'real' DC slack bus. However, in at least one of the nodes, the voltage needs to be regulated to ensure a safe operation of the DC grid, this can be either an IC operating in $V_{dc} - Q$ mode or a DC voltage node $\mathcal{M}_V$.

The generic PF equations for a hybrid, unbalanced AC/DC network are shown in (1). The model allows for multiple ICs with different operating modes [20]. Equations 1a - 1c model the *PQ* and *PV* nodes in the AC grid, equations 1d and 1e model the *P* and *V* nodes in DC network and equations 1g - 1j model the different operating modes of the ICs.

AC nodes

$$\Re\Big\{\overline{E}_i^{\phi} \sum\nolimits_{n\in\mathcal{N}} \underline{\mathbf{Y}}_{i,n}^{ac} \underline{\mathbf{E}}_n^{\phi}\Big\} = P_i^{\phi *}, \qquad \forall i \in \mathcal{N}_{PQ} \cup \mathcal{N}_{PV} \quad (1a)$$

$$\Im\Big\{\overline{E}_i^{\phi} \sum\nolimits_{n\in\mathcal{N}} \underline{\mathbf{Y}}_{i,n}^{ac} \underline{\mathbf{E}}_n^{\phi}\Big\} = Q_i^{\phi *}, \qquad \forall i \in \mathcal{N}_{PQ} \quad (1b)$$

$$(E_i^{\phi\prime})^2 + (E_i^{\phi\prime\prime})^2 = |E_i^{\phi *}|^2, \qquad \forall i \in \mathcal{N}_{PV} \quad (1c)$$

DC nodes

$$E_j \sum\nolimits_{m\in\mathcal{M}} Y_{j,m}^{dc} E_m = P_j^*, \qquad \forall j \in \mathcal{M}_P \quad (1d)$$

$$E_j = E_j^*, \qquad \forall j \in \mathcal{M}_V \quad (1e)$$

IC nodes

$$E_k^* \Big(Y_{(k,k)}^{dc} E_k^* + \sum\nolimits_{\substack{m\in\mathcal{M}\\ m\neq k}} Y_{(k,m)}^{dc} E_m\Big) = \Re\Big\{\overline{E}_l^{+} \sum\nolimits_{n\in\mathcal{N}} \underline{\mathbf{Y}}_{(l,n)}^{ac} \underline{\mathbf{E}}_n^{+}\Big\}, \quad \forall (l,k) \in \mathcal{L}_{V_{dc}Q} \quad (1f)$$

$$\Re\Big\{\overline{E}_l^{+} \sum\nolimits_{n\in\mathcal{N}} \underline{\mathbf{Y}}_{(l,n)}^{+ac} \underline{\mathbf{E}}_n^{+}\Big\} = P_l^*, \qquad \forall l \in \mathcal{L}_{PQ} \quad (1g)$$

$$\Im\Big\{\overline{E}_l^{+} \sum\nolimits_{n\in\mathcal{N}} \underline{\mathbf{Y}}_{(l,n)}^{+,ac} \underline{\mathbf{E}}_n^{+}\Big\} = Q_l^*, \qquad \forall l \in \mathcal{L}_{PQ} \cup \mathcal{L}_{V_{dc}Q} \quad (1h)$$

$$E_l^{0\prime} = 0, \quad E_l^{0\prime\prime} = 0, \qquad \forall l \in \mathcal{L}_{PQ} \cup \mathcal{L}_{V_{dc}Q} \quad (1i)$$

$$E_l^{n\prime} = 0, \quad E_l^{n\prime\prime} = 0, \qquad \forall l \in \mathcal{L}_{PQ} \cup \mathcal{L}_{V_{dc}Q} \quad (1j)$$

Where, ϕ is the phase: $\phi \in \{a, b, c\}$, the underbar $\underline{\square}$ indicates the complex conjugate. The prime symbols $\square'$ and $\square''$ refer to the real and imaginary parts of the complex electrical quantities. The subscripts $0, +, -$ denote the homopolar (zero), positive and negative sequence components following the standard symmetrical component decomposition. The asterisk $\square^*$ refers to the controllable variables.

IV. Methodology

Using the power flow model in (1) a closed-form mathematical expression is derived to compute the voltage SCs for the AC nodes, DC nodes and IC nodes in a unified way. In order not to lose the generality of the method, the voltage SCs are computed with respect to the set $\mathcal{X}$ controllable variables of the PF model (1). Furthermore, let x be any element from the set $\mathcal{X}$. Therefore,

$$\mathcal{X} = \Big\{P_i^{\phi *}, Q_i^{\phi *}, |\overline{E}_i^{\phi *}|, P_j^*, E_j^*, P_l^*, Q_l^*, E_k^*\Big\} \quad \forall\, i \in \mathcal{N}, \forall\, j \in \mathcal{M}, \forall\, (l,k) \in \mathcal{L} \quad (2)$$

In what follows, we derive the SCs with respect to each element in $\mathcal{X}$ using the procedure:

1) Compute the partial derivative with respect to $x \in \mathcal{X}$ of the PF equations (1).
2) Regroup the partial derivatives to obtain the linear system of equations $\mathbf{A}\ \mathbf{u}(x) = \mathbf{b}(x)$, where $\mathbf{u}(x)$ is the vector of the voltage SCs $\frac{\partial \overline{E}}{\partial x}$ as defined in (3).

$$\mathbf{u}(x) = \left[\frac{\partial \overline{E}_i^{\phi'}}{\partial x}, \frac{\partial \overline{E}_i^{\phi''}}{\partial x}, \frac{\partial E_j}{\partial x}, \frac{\partial \overline{E}_l^{\phi'}}{\partial x}, \frac{\partial \overline{E}_l^{\phi''}}{\partial x}, \frac{\partial E_k}{\partial x}\right] \quad \forall\, i \in \mathcal{N},\ j \in \mathcal{M},\ (l,k) \in \mathcal{L},\ \phi \in \{a,b,c\},\ x \in \mathcal{X} \quad (3)$$

3) Solve the linear system of equations to obtain $\mathbf{u}(x)$.

The assumptions made in the closed-form computation of the voltage SCs are reported below.

[2]The PF model only requires a lumped average model. Therefore, from the PF point of view, a two-level and a multi-level modular converter (MMC) are modelled identically. Only the converter losses and the filters are modelled differently. However, as any passive filter can be represented by a generic two-port equivalent circuit, we can easily incorporate the filter as an equivalent Π-equivalent branch model. Furthermore, a Current Source Converter CSC is modelled similarly to the VSC, except under unbalanced loading conditions as reported in [20]

- The voltage of the *Slack* bus $\overline{E}_s^{\phi}$ is fixed and can therefore, not be influenced by any control variables other than itself. Therefore,

$$\frac{\partial|\overline{E}_s^{\phi'}|}{\partial|\overline{E}_s^{\phi'}|}=1,\ \frac{\partial|\overline{E}_s^{\phi''}|}{\partial|\overline{E}_s^{\phi''}|}=1,\ \frac{\partial|\overline{E}_s^{\phi'}|}{\partial x}=0,\ \frac{\partial|\overline{E}_s^{\phi''}|}{\partial x}=0,\quad \forall\ x\in\mathcal{X} \tag{4}$$

  The voltage SCs of the slack node can be computed directly and is not required to be included in the linear system of equations. Therefore, the slack voltage is also not included in the set of controllable variables $\mathcal{X}$.
- Trivially, the partial derivative of any voltage with respect to itself is 1. This is relevant for the voltage-controllable nodes: the *PV* nodes in the AC grid, *V* nodes in the DC grid and the IC operating under $V_{dc}-Q$ mode.

$$\begin{aligned}\frac{\partial|\overline{E}_i^{\phi*}|}{\partial|\overline{E}_i^{\phi*}|}&=1, && \forall i\in\mathcal{N}_{PV},\\ \frac{\partial E_j^*}{\partial E_j^*}&=1, && \forall j\in\mathcal{M}_V,\\ \frac{\partial E_k^*}{\partial E_k^*}&=1, && \forall k\in\mathcal{L}_{V_{dc}Q}\end{aligned} \tag{5}$$

- We assume that the nodal voltage magnitudes of the voltage-controllable AC, DC and IC nodes are fixed and cannot be influenced by any other control variable. Therefore, the partial derivative of these voltages with respect to the other control variables equals zero.

$$\begin{aligned}\frac{\partial|\overline{E}_i^{\phi*}|}{\partial x}&=0, && \forall i\in\mathcal{N}_{PV},\ \forall x\in\mathcal{X}\setminus\{|\overline{E}_i^{\phi*}|\}\\ \frac{\partial E_j^*}{\partial x}&=0, && \forall j\in\mathcal{M}_V,\ \forall x\in\mathcal{X}\setminus\{E_j^*\}\\ \frac{\partial E_k^*}{\partial x}&=0, && \forall k\in\mathcal{L}_{V_{dc}Q},\ \forall x\in\mathcal{X}\setminus\{E_k^*\}\end{aligned} \tag{6}$$

Finally, the SC of a voltage in rectangular coordinates can be easily transformed to polar coordinates using the transformations in (7) and (8). In what follows, the SCs will be computed in the rectangular coordinate system.

$$\begin{aligned}\frac{\partial\overline{E}}{\partial x}&=\frac{\partial\overline{E}'}{\partial x}+j\frac{\partial\overline{E}''}{\partial x}=\overline{E}\left(\frac{1}{|\overline{E}|}\frac{\partial|\overline{E}|}{\partial x}+j\frac{\partial\angle\overline{E}}{\partial x}\right)\\ \frac{\partial\underline{E}}{\partial x}&=\frac{\partial\overline{E}'}{\partial x}-j\frac{\partial\overline{E}''}{\partial x}=\underline{E}\left(\frac{1}{|\overline{E}|}\frac{\partial|\overline{E}|}{\partial x}-j\frac{\partial\angle\overline{E}}{\partial x}\right)\end{aligned} \tag{7}$$

and,

$$\frac{\partial|\overline{E}|}{\partial x}=\frac{1}{|\overline{E}|}\Re\left\{\underline{E}\frac{\partial\overline{E}}{\partial x}\right\}\ \text{and}\ \frac{\partial\angle\overline{E}}{\partial x}=\frac{1}{|\overline{E}|^2}\Im\left\{\underline{E}\frac{\partial\overline{E}}{\partial x}\right\} \tag{8}$$

Furthermore, to improve the clarity of this paper, the expressions $\phi\in\{a,b,c\}$ and $x\in\mathcal{X}$ are omitted from every equation below, but are valid.

A. Voltage SC in the AC grid

In the generic case, the voltage SCs for the *PQ* and *PV* nodes in the AC grid with respect to x are computed starting from the power flow equation (1a) and (1b) that relate the power injection to the nodal voltages.

$$P_i^{\phi*}+jQ_i^{\phi*}=\overline{E}_i^{\phi}\sum_{n\in\mathcal{N}}\underline{\mathbf{Y}}_{i,n}^{ac}\underline{\mathbf{E}}_n^{\phi},\qquad \forall i\in\mathcal{N}_{PQ} \tag{9}$$

Next, we take the partial derivative of (9) with respect to x.

$$\frac{\partial P_i^{\phi*}}{\partial x}+j\frac{\partial Q_i^{\phi*}}{\partial x}=\overline{E}_i^{\phi}\frac{\partial}{\partial x}\left(\sum_{n\in\mathcal{N}}\underline{\mathbf{Y}}_{i,n}^{ac}\underline{\mathbf{E}}_n^{\phi}\right)+\frac{\partial\overline{E}_i^{\phi}}{\partial x}\sum_{n\in\mathcal{N}}\underline{\mathbf{Y}}_{i,n}^{ac}\underline{\mathbf{E}}_n^{\phi}\qquad \forall i\in\mathcal{N}_{PQ} \tag{10}$$

Using the identities in (7), we can reformulate (10) into its real and imaginary components. Furthermore, because $\overline{E}_i^{\phi}$ in the first term is not dependent on n, we can bring it into the summation.

$$\begin{aligned}\frac{\partial P_i^{\phi*}}{\partial x}+j\frac{\partial Q_i^{\phi*}}{\partial x}=&\sum_{n\in\mathcal{N}}\overline{E}_i^{\phi}\underline{\mathbf{Y}}_{i,n}^{ac}\left(\frac{\partial\overline{E}_n^{\phi'}}{\partial x}-j\frac{\partial\overline{E}_n^{\phi''}}{\partial x}\right)\\ &+\left(\frac{\partial\overline{E}_i^{\phi'}}{\partial x}-j\frac{\partial\overline{E}_i^{\phi''}}{\partial x}\right)\sum_{n\in\mathcal{N}}\underline{\mathbf{Y}}_{i,n}^{ac}\underline{\mathbf{E}}_n^{\phi}\end{aligned} \tag{11}$$

Expression (11) can be simplified by substituting:

$$\overline{F}_{i,n}^{\phi}=\overline{E}_i^{\phi}\underline{\mathbf{Y}}_{i,n}^{ac}\quad\text{and}\quad\overline{H}_i^{\phi}=\sum_{n\in\mathcal{N}}\underline{\mathbf{Y}}_{i,n}^{ac}\underline{\mathbf{E}}_n^{\phi} \tag{12}$$

Substituting (12) in (11) and rearranging the real and imaginary terms, gives the expression for the active and reactive power injections that is linear in $\frac{\partial E}{\partial x}$.

$$\begin{aligned}\frac{\partial P_i^{\phi*}}{\partial x}=&\left(\overline{F}_{i,i}^{\phi'}+\overline{H}_i^{\phi'}\right)\frac{\partial\overline{E}_i^{\phi'}}{\partial x}+\sum_{n\in\mathcal{N}\setminus\{i\}}\overline{F}_{i,n}^{\phi'}\frac{\partial\overline{E}_n^{\phi'}}{\partial x}\\ &+\left(\overline{F}_{i,i}^{\phi''}-\overline{H}_i^{\phi''}\right)\frac{\partial\overline{E}_i^{\phi''}}{\partial x}+\sum_{n\in\mathcal{N}\setminus\{i\}}\overline{F}_{i,n}^{\phi''}\frac{\partial\overline{E}_n^{\phi''}}{\partial x}\\ &\forall i\in\mathcal{N}_{PQ}\cup\mathcal{N}_{PV}\end{aligned} \tag{13}$$

$$\begin{aligned}\frac{\partial Q_i^{\phi*}}{\partial x}=&\left(\ \overline{F}_{i,i}^{\phi''}+\overline{H}_i^{\phi''}\right)\frac{\partial\overline{E}_i^{\phi'}}{\partial x}+\sum_{n\in\mathcal{N}\setminus\{i\}}\overline{F}_{i,n}^{\phi'}\frac{\partial\overline{E}_n^{\phi'}}{\partial x}\\ &+\left(-\overline{F}_{i,i}^{\phi'}+\overline{H}_i^{\phi'}\right)\frac{\partial\overline{E}_i^{\phi''}}{\partial x}-\sum_{n\in\mathcal{N}\setminus\{i\}}\overline{F}_{i,n}^{\phi''}\frac{\partial\overline{E}_n^{\phi''}}{\partial x}\\ &\forall i\in\mathcal{N}_{PQ}\end{aligned} \tag{14}$$

The voltage SCs of the PV nodes in the AC grid are computed starting from the PF model (1c) that relates the voltage magnitude to its real and imaginary part.

$$|\overline{E}_i^{\phi*}|^2=(\overline{E}_i^{\phi'})^2+(\overline{E}_i^{\phi''})^2,\quad\forall i\in\mathcal{N}_{PV} \tag{15}$$

Next, we take the partial derivative of (15) with respect to x to obtain the linear expression of the voltage sensitivity coefficients.

$$|\overline{E}_i^{\phi*}|\frac{\partial|\overline{E}_i^{\phi*}|}{\partial x}=\overline{E}_i^{\phi'}\frac{\partial\overline{E}_i^{\phi'}}{\partial x}+\overline{E}_i^{\phi''}\frac{\partial\overline{E}_i^{\phi''}}{\partial x},\ \forall i\in\mathcal{N}_{PV} \tag{16}$$

B. Voltage SC in the DC grid

The DC grid model distinguishes *P* nodes ($\mathcal{M}_P$) and *V* nodes ($\mathcal{M}_V$). Because of its DC nature, all the electrical quantities are real: $\overline{E}_j=E_j,\ \forall j\in\mathcal{M}$.

The power injection in the DC node j is expressed as presented in the PF model (1d),

$$P_j^*=E_j\sum_{m\in\mathcal{M}}Y_{j,m}^{dc}E_m,\qquad\forall j\in\mathcal{M}_P \tag{17}$$

The voltage SCs are computed by taking the partial derivative of equation (17) to x.

$$\frac{\partial P_j^*}{\partial x} = E_j \sum_{m\in\mathcal{M}} Y_{j,m}^{dc} \frac{\partial E_m}{\partial x} + \frac{\partial E_j}{\partial x} \sum_{m\in\mathcal{M}} Y_{j,m}^{dc} E_m \qquad \forall j \in \mathcal{M}_P \tag{18}$$

Using the identities in (19), the expression (18) is simplified to (20)

$$F_{j,m} = E_j Y_{j,m}^{dc} \quad \text{and} \quad H_j = \sum_{m\in\mathcal{M}} Y_{j,m}^{dc} E_m \tag{19}$$

$$\frac{\partial P_j^*}{\partial x} = (F_{j,j} + H_j) \frac{\partial E_j}{\partial x} + \sum_{m\in\mathcal{M}\setminus\{j\}} F_{j,m} \frac{\partial E_m}{\partial x} \qquad \forall j \in \mathcal{M}_P \tag{20}$$

The voltage SCs of the *V* nodes are formulated in (21).

$$\frac{\partial E_j^*}{\partial x} = \frac{\partial E_j}{\partial x}, \qquad \forall j \in \mathcal{M}_V \tag{21}$$

C. Voltage SC for the Interfacing Converters

Finally, the expressions of the partial derivatives of the IC's voltages are formulated to be included in the unified closed-form SC model. Every IC is connected to a node pair $(k,l) \in \mathcal{L}$, where l is the IC's AC node and k is the IC's DC node. To improve the clarity of the model, first, the system of equations is derived for balanced grid conditions. In the next section (IV-D), the SC model is adapted for unbalanced grid conditions.

For the IC's operating mode $\mathbf{V_{dc} - Q}$, the SCs are computed starting from the PF equations described in (1f) and (1h). The model relating the controllable DC voltage to the other AC and DC nodal voltages is given in (22).

$$\Re\Big\{\overline{E}_l^{\phi} \sum_{n\in\mathcal{N}} \underline{Y}_{(l,n)}^{ac} \underline{E}_n\Big\} = E_k^{\phi *}\Big(Y_{(k,k)}^{dc} E_k^* + \sum_{m\in\mathcal{M}\setminus\{k\}} Y_{(k,m)}^{dc} E_m\Big) \qquad \forall (l,k) \in \mathcal{L}_{V_{dc}Q} \tag{22}$$

Next, we take the partial derivative of (22) to x. The derivative of the left-hand side of (22) is computed analogously to (12), however, the indices have to be suitably adapted to the IC's AC node l. The derivative of the right-hand side reads:

$$\frac{\partial E_k^*}{\partial x}\Big(Y_{(k,k)}^{dc} E_k^* + \sum_{m\in\mathcal{M}\setminus\{k\}} Y_{(k,m)}^{dc} E_m\Big) + E_k^*\Big(Y_{(k,k)}^{dc} \frac{\partial E_k^*}{\partial x} + \sum_{m\in\mathcal{M}\setminus\{k\}} Y_{(k,m)}^{dc} \frac{\partial E_m}{\partial x}\Big) \tag{23}$$

Finally, we regroup the terms to obtain a linear relation of the partial derivative of the controllable DC voltage $\frac{\partial E_k^*}{\partial x}$. Furthermore, the expression is simplification using (19).

$$\Big(F_{(k,k)} + H_k\Big)\frac{\partial E_k^*}{\partial x} = -\sum_{m\in\mathcal{M}\setminus\{k\}} F_{(k,m)} \frac{\partial E_m}{\partial x} + \Big(\overline{F}_{l,l}^{\phi'} + \overline{H}_l^{\phi'}\Big)\frac{\partial \overline{E}_l^{\phi'}}{\partial x} + \sum_{n\in\mathcal{N}\setminus\{l\}} \overline{F}_{l,n}^{\phi'} \frac{\partial \overline{E}_n^{\phi'}}{\partial x} + \Big(\overline{F}_{l,l}^{\phi''} - \overline{H}_l^{\phi''}\Big)\frac{\partial \overline{E}_l^{\phi''}}{\partial x} + \sum_{n\in\mathcal{N}\setminus\{l\}} \overline{F}_{l,n}^{\phi''} \frac{\partial \overline{E}_n^{\phi''}}{\partial x} \qquad \forall (l,k) \in \mathcal{L}_{V_{dc}Q} \tag{24}$$

For the operating mode $\mathbf{P - Q}$, the partial derivatives of the **active power** injections of the ICs into the AC grid are described similarly to (13).

$$\frac{\partial P_l^{\phi *}}{\partial x} = \Big(\overline{F}_{l,l}^{\phi'} + \overline{H}_l^{\phi'}\Big)\frac{\partial \overline{E}_l^{\phi'}}{\partial x} + \sum_{n\in\mathcal{N}\setminus\{i\}} \overline{F}_{l,n}^{\phi'} \frac{\partial \overline{E}_n^{\phi'}}{\partial x} + \Big(\overline{F}_{l,l}^{\phi''} - \overline{H}_l^{\phi''}\Big)\frac{\partial \overline{E}_l^{\phi''}}{\partial x} + \sum_{n\in\mathcal{N}\setminus\{l\}} \overline{F}_{l,n}^{\phi''} \frac{\partial \overline{E}_n^{\phi''}}{\partial x} \qquad \forall l \in \mathcal{L}_{PQ} \tag{25}$$

Typically, the ICs operating in $P - Q$ mode, are given an AC power reference to track. Using the active power balance at the IC between the AC and the DC network, we can say that $P_l^{\phi *} = P_k^*$. Therefore, the partial derivatives of the active power injected into the DC grid is described in (26)

$$\frac{\partial P_k^*}{\partial x} = (F_{k,k} + H_k)\frac{\partial E_k}{\partial x} + \sum_{m\in\mathcal{M}\setminus\{k\}} F_{k,m} \frac{\partial E_m}{\partial x} \qquad \forall k \in \mathcal{L}_{V_{dc}Q} \tag{26}$$

The **reactive power** injection of the IC is described identically to equation (14), where the indices are suitably adapted. Therefore, the linear SC model for the reactive power injection in both the $P - Q$ and the $V_{dc} - Q$ operating mode is given by (27).

$$\frac{\partial Q_l^{\phi *}}{\partial x} = \Big(\ \overline{F}_{l,l}^{\phi''} + \overline{H}_l^{\phi''}\Big)\frac{\partial \overline{E}_l^{\phi'}}{\partial x} + \sum_{n\in\mathcal{N}\setminus\{l\}} \overline{F}_{l,n}^{\phi''} \frac{\partial \overline{E}_n^{\phi'}}{\partial x} + \Big(-\overline{F}_{l,l}^{\phi'} + \overline{H}_l^{\phi'}\Big)\frac{\partial \overline{E}_l^{\phi''}}{\partial x} - \sum_{n\in\mathcal{N}\setminus\{l\}} \overline{F}_{l,n}^{\phi'} \frac{\partial \overline{E}_n^{\phi''}}{\partial x} \qquad \forall l \in \mathcal{L}_{V_{dc}Q} \cup \mathcal{L}_{PQ} \tag{27}$$

D. Unbalanced loading conditions

For unbalanced loading conditions, the linear SC model described by equations (13), (14), (16), (20), (21), (24), (25), (26) and (27) has to be adapted accordingly. The linear equations for the AC and DC system are written for each phase individually, and therefore, remain the same. Only the expressions of the IC's models have to be adapted. The PLL of each IC typically synchronizes with the positive sequence component of the AC grid's voltage. Therefore, the voltage's zero and negative sequence components are zero at the AC terminal and, therefore, the ICs only inject positive sequence power.

Using the Fortescue transformation, we decompose the three-phase voltages and currents into their symmetrical components as shown in (28) [3]. $\overline{\mathbf{E}}^{0+-} = [\overline{E}^0\ \overline{E}^+\ \overline{E}^-]^\intercal$ is the vector containing the zero, positive and negative sequence component of the nodal voltage phasor, $\overline{\mathbf{T}}$ is the transformation matrix, $\overline{\mathbf{E}}^{abc} = [\overline{E}^a\ \overline{E}^b\ \overline{E}^c]^\intercal$ and $\alpha = e^{\frac{2}{3}\pi j}$.

$$\overline{\mathbf{E}}^{0+-} = \overline{\mathbf{T}}\overline{\mathbf{E}}^{abc} \quad \text{with,} \quad \overline{\mathbf{T}} = \frac{1}{3}\begin{bmatrix} 1 & 1 & 1 \\ 1 & \alpha & \alpha^2 \\ 1 & \alpha^2 & \alpha \end{bmatrix} \tag{28}$$

For the $\mathbf{V_{dc} - Q}$ operating mode, the PF model is adapted in (29) for unbalanced loading conditions. Because the ICs

[3]The symmetrical component transformation requires the assumption that the lines' admittance matrices are circular symmetric.

only inject the positive sequence power, the active power balance between the AC and DC part is based on the positive sequence voltage $\overline{E}^{+}$.

$$\Re\Big\{\overline{E}_l^{+}\sum\nolimits_{n\in\mathcal{N}}\underline{Y}_{(l,n)}^{ac}\underline{E}_n^{+}\Big\}=E_k^{*}\Big(Y_{(k,k)}^{dc}E_k^{*}+\sum_{m\in\mathcal{M}\setminus\{k\}}Y_{(k,m)}^{dc}E_m\Big)\quad\forall(l,k)\in\mathcal{L}_{V_{dc}Q}\tag{29}$$

If we take the partial derivative of (29) to x, we obtain a linear expression in $\frac{\partial\overline{E}^{+}}{\partial x}$. However, the partial derivative of the positive sequence voltages are not part of the vector of unknowns in (3). Therefore, $\frac{\partial\overline{E}^{+}}{\partial x}$ in (29) has to be transformed again to its phase domain to obtain a linear expression dependent only on the unknowns of (3).

We transform the identities $\overline{F}$ and $\overline{H}$ to their sequence domain as shown in (30). Because of the unbalanced nature, the three phases cannot be treated individually anymore, but the electrical quantities become vectors. Therefore, the identities $\overline{\mathbf{F}}_{i,n}^{0+-}$ and $\overline{\mathbf{H}}_{i}^{0+-}$ are 3-by-3 matrices where every row refers to the zero, positive and negative sequence components. Furthermore, we use the notation where $\overline{\mathbf{F}}_{i,n}^{0}$ is the first row related to the homopolar sequence, $\overline{\mathbf{F}}_{i,n}^{+}$ is the second row related to the positive sequence and $\overline{\mathbf{F}}_{i,n}^{-}$ is the third row related to the negative sequence. The partial derivative of the vector $\overline{\mathbf{E}}^{abc}$ to x is equal to $\frac{\partial\overline{\mathbf{E}}^{abc}}{\partial x}=\left[\frac{\partial\overline{E}^{a}}{\partial x},\frac{\partial\overline{E}^{b}}{\partial x},\frac{\partial\overline{E}^{c}}{\partial x}\right]^{\mathsf{T}}$.

$$\begin{aligned}\overline{\mathbf{F}}_{i,n}^{0+-}&=\overline{\mathbf{T}}^{-1}\mathrm{diag}(\underline{\mathbf{Y}}_{i,n}^{ac}\overline{\mathbf{T}}\overline{\mathbf{E}}_i^{abc})\\ \overline{\mathbf{H}}_{i}^{0+-}&=\overline{\mathbf{T}}^{-1}\mathrm{diag}(\sum_{n\in\mathcal{N}}\underline{\mathbf{Y}}_{i,n}^{ac}\underline{\mathbf{T}}\overline{\mathbf{E}}_i^{abc})\end{aligned}\tag{30}$$

Next, using the above identities, a linear expression of the phase-domain partial derivatives, $\frac{\partial\overline{E}^{\phi}}{\partial x}$, is formulated for the ICs operating in $V_{dc}-Q$ mode (31).

$$\begin{aligned}\Big(F_{(k,k)}+H_k\Big)\frac{\partial E_k^{*}}{\partial x}=&-\sum_{m\in\mathcal{M}\setminus\{k\}}F_{(k,m)}\frac{\partial E_m}{\partial x}\\&+\Big(\overline{\mathbf{F}}_{l,l}^{+'}+\overline{\mathbf{H}}_{i}^{+'}\Big)\frac{\partial\overline{\mathbf{E}}_l^{abc'}}{\partial x}+\Big(\sum_{n\in\mathcal{N}\setminus\{l\}}\overline{\mathbf{F}}_{l,n}^{+'}\Big)\frac{\partial\overline{\mathbf{E}}_n^{abc'}}{\partial x}\\&+\Big(\overline{\mathbf{F}}_{l,l}^{+''}-\overline{\mathbf{H}}_{i}^{+''}\Big)\frac{\partial\overline{\mathbf{E}}_l^{abc''}}{\partial x}+\Big(\sum_{n\in\mathcal{N}\setminus\{l\}}\overline{\mathbf{F}}_{l,n}^{+''}\Big)\frac{\partial\overline{\mathbf{E}}_n^{abc''}}{\partial x}\\&\forall(l,k)\in\mathcal{L}_{V_{dc}Q}\end{aligned}\tag{31}$$

Furthermore, because the ICs only inject the positive sequence powers, the negative and zero sequence powers are zero. As explained in [20], formulating the linear system of equations using the partial derivative of the zero and negative power injection, results in the trivial expression and thus an undetermined problem. Therefore, the derivation of the SC model starts from expressions (1i) and (1j) that are reformulated into the phase-domain as shown in (32):

$$\overline{E}_l^{0'}=\overline{\mathbf{T}}^{0'}\overline{\mathbf{E}}_l^{abc'}-\overline{\mathbf{T}}^{0''}\overline{\mathbf{E}}_l^{abc''}=0,\tag{32a}$$

$$\overline{E}_l^{-'}=\overline{\mathbf{T}}^{-'}\overline{\mathbf{E}}_l^{abc'}-\overline{\mathbf{T}}^{-''}\overline{\mathbf{E}}_l^{abc''}=0,\quad\forall l\in\mathcal{L}_{V_{dc}Q}\cup\mathcal{L}_{PQ}\tag{32b}$$

where e.g. $\overline{\mathbf{T}}^{0'}$ refers to the row of the transformation matrix that corresponds to the zero sequence. Taking the partial derivative of (32) gives the linear expression:

$$\overline{\mathbf{T}}^{0'}\frac{\partial\overline{\mathbf{E}}_l^{abc'}}{\partial x}-\overline{\mathbf{T}}^{0''}\frac{\partial\overline{\mathbf{E}}_l^{abc''}}{\partial x}=0,\tag{33a}$$

$$\overline{\mathbf{T}}^{-'}\frac{\partial\overline{\mathbf{E}}_l^{abc'}}{\partial x}-\overline{\mathbf{T}}^{-''}\frac{\partial\overline{\mathbf{E}}_l^{abc''}}{\partial x}=0,\quad\forall l\in\mathcal{L}_{V_{dc}Q}\cup\mathcal{L}_{PQ}\tag{33b}$$

For the $\mathbf{P}-\mathbf{Q}$ operating mode, equation (25) is similarly adapted for unbalanced conditions. In the case that the IC is only injecting positive sequence power, SC model for the active power injection consists of (34) and the linear equations in (33) to describe the zero and negative power injection.

$$\begin{aligned}\frac{\partial P_l^{p*}}{\partial x}=&\Big(\overline{\mathbf{F}}_{l,l}^{+'}+\overline{\mathbf{H}}_{i}^{+'}\Big)\frac{\partial\overline{\mathbf{E}}_l^{abc'}}{\partial x}+\Big(\sum_{n\in\mathcal{N}\setminus\{l\}}\overline{\mathbf{F}}_{l,n}^{+'}\Big)\frac{\partial\overline{\mathbf{E}}_n^{abc'}}{\partial x}\\&+\Big(\overline{\mathbf{F}}_{l,l}^{+''}-\overline{\mathbf{H}}_{i}^{+''}\Big)\frac{\partial\overline{\mathbf{E}}_l^{abc''}}{\partial x}+\Big(\sum_{n\in\mathcal{N}\setminus\{l\}}\overline{\mathbf{F}}_{l,n}^{+''}\Big)\frac{\partial\overline{\mathbf{E}}_n^{abc''}}{\partial x}\\&\forall l\in\mathcal{L}_{PQ}\end{aligned}\tag{34}$$

The reactive power injections of both operation modes of the IC under unbalanced conditions is formulated in (35).

$$\begin{aligned}\frac{\partial Q_l^{\phi*}}{\partial x}=&\Big(\overline{\mathbf{F}}_{l,l}^{+''}+\overline{\mathbf{H}}_{i}^{+''}\Big)\frac{\partial\overline{\mathbf{E}}_l^{abc'}}{\partial x}+\Big(\sum_{n\in\mathcal{N}\setminus\{l\}}\overline{\mathbf{F}}_{l,n}^{+''}\Big)\frac{\partial\overline{\mathbf{E}}_n^{abc'}}{\partial x}\\&+\Big(\overline{\mathbf{F}}_{l,l}^{+'}-\overline{\mathbf{H}}_{i}^{+'}\Big)\frac{\partial\overline{\mathbf{E}}_l^{abc''}}{\partial x}+\Big(\sum_{n\in\mathcal{N}\setminus\{l\}}\overline{\mathbf{F}}_{l,n}^{+'}\Big)\frac{\partial\overline{\mathbf{E}}_n^{abc''}}{\partial x}\end{aligned}\tag{35a}$$

$$\overline{\mathbf{T}}^{0''}\frac{\partial\overline{\mathbf{E}}_l^{abc'}}{\partial x}+\overline{\mathbf{T}}^{0'}\frac{\partial\overline{\mathbf{E}}_l^{abc''}}{\partial x}=0\tag{35b}$$

$$\overline{\mathbf{T}}^{-''}\frac{\partial\overline{\mathbf{E}}_l^{abc'}}{\partial x}+\overline{\mathbf{T}}^{-'}\frac{\partial\overline{\mathbf{E}}_l^{abc''}}{\partial x}=0\quad\forall l\in\mathcal{L}_{V_{dc}Q}\cup\mathcal{L}_{PQ}\tag{35c}$$

In the specific case that the IC control also allows intentionally negative power injection, equations (34) and (35) are reformulated for the negative sequence to replace (33b) and (35c).

E. Linear system of equations

The closed-form SC model for hybrid AC/DC networks is formulated as equations (13), (14), (16), (20), (21), (24), (26), (31), (33), (34) and (35). Regrouping these equations results in a system of equations that is linear with respect to the partial derivatives of the voltage (3). The model is formulated as $\mathbf{A}\ \mathbf{u}(x)=\mathbf{b}(x)$.

The matrix $\mathbf{A}$ is defined in (36) as a 7×7 block matrix, one for each type of node in the AC grid, DC grid and ICs. The rows represent the linearized PF equations derived above. The columns represent the individual terms of each linearized PF equation, grouped per node type. The matrix $\mathbf{A}$ only depends on the state of the grid i.e., the nodal voltage at every node, and the admittance matrix. Furthermore, it is independent of

the control variables $x \in \mathcal{X}$ and thus has to be computed only once. We do not give explicitly the expressions for A_{ij} since they are trivially derived from (13), (14), (16), (20), (21), (24), (26), (31), (33), (34) and (35). In Appendix A, a detailed numerical example of the construction of the matrix $\mathbf{A}$ is given for a 5-node example grid.

$$
\begin{array}{c}
\overbrace{\qquad\qquad}^{\text{AC nodes}}\ \overbrace{\qquad}^{\text{DC nodes}}\ \overbrace{\qquad\qquad\qquad}^{\text{IC nodes}} \\
\begin{array}{cc|cc|c|c|cc|cc|c}
\multicolumn{2}{c|}{\overbrace{\mathcal{N}_{PQ}}} & \multicolumn{2}{c|}{\overbrace{\mathcal{N}_{PV}}} & \overbrace{\mathcal{M}_P} & \overbrace{\mathcal{M}_V} & \multicolumn{2}{c|}{\overbrace{\mathcal{L}_{l,PQ}}} & \multicolumn{2}{c|}{\overbrace{\mathcal{L}_{V_{dc}Q}}} & \overbrace{\mathcal{L}_{k,PQ}} \\
\frac{\partial E_i^{\phi'}}{\partial \mathcal{X}} & \frac{\partial E_i^{\phi''}}{\partial \mathcal{X}} & \frac{\partial E_i^{\phi'}}{\partial \mathcal{X}} & \frac{\partial E_i^{\phi''}}{\partial \mathcal{X}} & \frac{\partial E_j}{\partial \mathcal{X}} & \frac{\partial E_i^{\phi''}}{\partial \mathcal{X}} & \frac{\partial E_l^{\phi'}}{\partial \mathcal{X}} & \frac{\partial E_l^{\phi''}}{\partial \mathcal{X}} & \frac{\partial E_l^{\phi'}}{\partial \mathcal{X}} & \frac{\partial E_l^{\phi''}}{\partial \mathcal{X}} & \frac{\partial E_k}{\partial \mathcal{X}} \\
\hline
A_{11} & A_{12} & A_{13} & A_{14} & A_{15} & A_{16} & A_{17} & \} \mathcal{N}_{PQ} \\
A_{21} & A_{22} & A_{23} & A_{24} & A_{25} & A_{26} & A_{27} & \} \mathcal{N}_{PV} \\
\hdashline
A_{31} & A_{32} & A_{33} & A_{34} & A_{35} & A_{36} & A_{37} & \} \mathcal{M}_P \\
A_{41} & A_{42} & A_{43} & A_{44} & A_{45} & A_{46} & A_{47} & \} \mathcal{M}_V \\
\hdashline
A_{51} & A_{52} & A_{53} & A_{54} & A_{55} & A_{56} & A_{57} & \} \mathcal{L}_{l,PQ} \\
A_{61} & A_{62} & A_{63} & A_{64} & A_{65} & A_{66} & A_{67} & \} \mathcal{L}_{V_{dc}Q} \\
A_{71} & A_{72} & A_{73} & A_{74} & A_{75} & A_{76} & A_{77} & \} \mathcal{L}_{k,PQ}
\end{array}
\end{array}
\tag{36}
$$

The vector $\mathbf{b}$, shown in (37), is unique for every control variable x. The vector is constructed by substituting x in the left-hand side of (13), (14), (16), (20), (21), (24), (26), (31), (33), (34) and (35) for every control variable. Because the construction of $\mathbf{b}(x)$ is unique for every control variable, the different vectors are not be explicitly given due to space limitations. However, a numerical example is given in Appendix A and the full model has been made publically available on https://github.com/DESL-EPFL.

$$
\mathbf{b}(x) = \begin{bmatrix}
b_1(x) & \} \mathcal{N}_{PQ} \\
b_2(x) & \} \mathcal{N}_{PV} \\
\hdashline
b_3(x) & \} \mathcal{M}_P \\
b_4(x) & \} \mathcal{M}_V \\
\hdashline
b_5(x) & \} \mathcal{L}_{l,PQ} \\
b_6(x) & \} \mathcal{L}_{V_{dc}Q} \\
b_7(x) & \} \mathcal{L}_{k,PQ}
\end{bmatrix}
\tag{37}
$$

***Corollary** 1:* The analytical model for the computation of the SCs for hybrid AC/DC grids, given by equations (13), (14), (16), (20), (21), (24), (26), (31), (33), (34) and (35) has a unique solution in any operating point where the PF model's Jacobian of the hybrid AC/DC network is invertible. This follows directly from the theorem in [23] that proves the uniqueness of the solution of the SCs for a solely AC network. The proof of the corollary is given in Appendix B.

It is interesting to mention that the SCs are inherently a property of the system. They are only dependent on the state of the network, the network's admittance matrix and the type of node, i.e. if the control variable is a voltage or a power.

Furthermore, the converter and resource limits are not influencing the computation of the SCs. This is because the PF model, used to derive the SCs, can be represented as a continuous hyperplane in the n-dimensional space, that is locally linearized. Therefore, the converter limits are simply a constraint that can be applied a posteriori in this n-dimensional space to upperbound the converters and resource setpoints, and has accordingly no impact on the SCs.

F. Current sensitivity coefficients

Using the voltage SCs and assuming the knowledge of the systems admittance matrix, we derive all other SCs, such as the branch currents, current injections, sequence voltages/currents and line losses. Below, the branch current sensitivity coefficients are computed using the Π-equivalent line model (see Figure 2). The AC current flow between the buses i and n and the DC current flow between buses j and m is expressed as:

$$
\begin{aligned}
\bar{I}_{i,n} &= \overline{Y}^{ac}_{(i,n),L} \left(\overline{E}_i - \overline{E}_n\right) + \overline{Y}^{ac}_{(i,n),T_i} \overline{E}_i, \\
I_{j,m} &= Y^{dc}_{(j,m),L} \left(E_j - E_m\right),
\end{aligned}
\tag{38}
$$

where the complex voltage SC are computed using (7). Therefore, the branch current sensitivity coefficients are described in (40).

$$
\frac{\partial \bar{I}_{i,n}}{\partial x} = \overline{Y}^{ac}_{(i,n),L} \left(\frac{\partial \overline{E}_i}{\partial x} - \frac{\partial \overline{E}_n}{\partial x}\right) + \overline{Y}^{ac}_{(i,n),T_i} \frac{\partial \overline{E}_i}{\partial x} \tag{39}
$$

$$
\frac{\partial I_{j,m}}{\partial x} = Y^{dc}_{(j,m),L} \left(\frac{\partial E_j}{\partial x} - \frac{\partial E_m}{\partial x}\right) \tag{40}
$$

V. Numerical validation

The proposed analytical method is benchmarked against two different numerical methods: 1) a perturb-and-observe-based method and 2) a method based on the inversion of the Jacobian of the solved load flow[4].

The perturbation-based validation method follows a perturb-and-observe strategy where a small perturbation is individually applied to each controllable variable. This process is repeated for every node in the system, i.e. all the *PQ*-nodes, *PV*-nodes, *P*-nodes, *V*-nodes and the *IC*-nodes. The state of the network is computed before and after the perturbation and the numerical SCs are derived as in (41).

$$
\frac{\Delta \overline{E}_i'}{\Delta x} = \frac{\overline{E}_i^{t_0} - \overline{E}_i^{t_1}}{x^{t_0} - x^{t_1}} \qquad \forall x \in \mathcal{X}, i \in \mathcal{N} \tag{41a}
$$

$$
\frac{\Delta E_j'}{\Delta x} = \frac{E_j^{t_0} - E_i^{t_1}}{x^{t_0} - x^{t_1}} \qquad \forall x \in \mathcal{X}, j \in \mathcal{M}, \tag{41b}
$$

where $t = t_0$ is before the perturbation and $t = t_1$ is after when the system reaches its post-perturbation steady-state[5].

The second validation method is based on the inversion of the Jacobian of the solved load flow. As described in Section I, the Jacobian-based method only allows to validate the SCs of the power-dependent nodes (active and reactive). The SC of the voltage-dependent nodes, i.e. where $x = E_l \ \forall l \in \mathcal{L}_{V_{dc}Q}$, $x = E_j \ \forall j \in \mathcal{M}_P$ and $x = |\overline{E}_i| \ \forall i \in \mathcal{N}_{PV}$ can only be validated using the perturbation-based method. The two methods are

[4]Because no other method for the computation of the SC for hybrid multiterminal AC/DC networks has been presented in the literature, we cannot benchmark our proposed method against any other method.

[5]The value of t_1 is case-dependent and assessed by the user as a function of the perturbation type and its location.

considered as the 'ground truth' for the benchmarking of the proposed analytical method. The metrics used to quantify the accuracy levels of the proposed method are the RMSE (root mean squared error) and the maximum error of all voltage SCs either on the real or imaginary part. The numerical validation is performed on a 26-node hybrid AC/DC low-voltage microgrid under balanced and unbalanced loading conditions (Section V-A) and on a multiterminal HVDC grid that interconnects two non-synchronous AC transmission grid (Section V-B).

A. Hybrid AC/DC microgrid

The topology of the 26-node hybrid AC/DC grid is shown in Figure 3. The grid consists of the low voltage AC CIGRE benchmark grid [24] that is suitably extended with a DC grid. The AC network consists of 18 nodes and has a base voltage of 400 V. The DC grid consists of 8 nodes and has a base voltage of 800 V. The base power for both networks is 100 kW. Table II summarises the node types and IC's operating modes of the hybrid network. The line parameters of the grid are shown in Table III. Further information about the hybrid grid and its resources is given in [25].

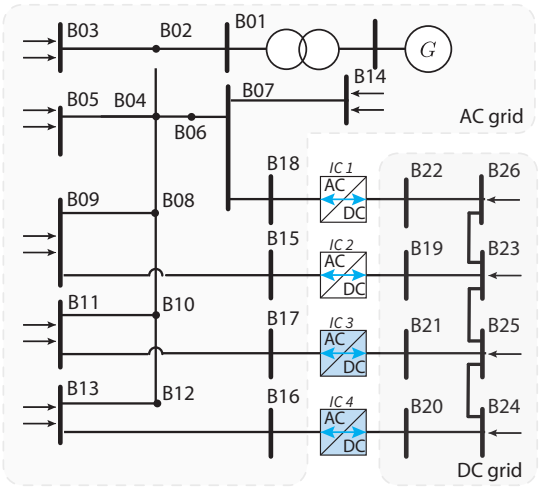

Fig. 3: Topology of the hybrid 26-node AC/DC microgrid.

TABLE II: Node types in the hybrid AC/DC microgrid

AC	
Bus Type	**Bus #**
PQ	2-14
VSC ($E_{dc} - Q_{ac}$)	15,18
VSC (P_{ac} - Q_{ac})	16,17
AC slack	1

DC	
Bus Type	**Bus #**
P	24-26
VSC ($E_{dc} - Q_{ac}$)	19,20
VSC (P_{ac} - Q_{ac})	21,22

The hybrid microgrid with the different ICs is modelled in a time-domain model in the EMTP-RV simulation environment[6] [26]. The loads in the AC and DC networks are represented as constant power loads. The boundary conditions of the simulation, i.e. the power injections in the P(Q) nodes and the voltage profile in (P)V and IC nodes, are sampled from real measurements of the hybrid AC/DC microgrid that is available at the Distributed Electrical System Laboratory (DESL) at the EPFL. The proposed SC computation method is validated for balanced and unbalanced loading conditions. The unbalanced conditions are generated by injecting a difference of 0.5 p.u. between the phases of bus $B09$.

[6]The simulation model is made publicly available on the DESL GitHub pagehttps://github.com/DESL-EPFL

TABLE III: Line parameters of the hybrid 26-node AC/DC microgrid.

Line	**R** (Ω/km)	**X** (Ω/km)	**B** (μS/km)	**Amp.** (A)	**Length** (m)
1 - 2	0.27	0.119	100.5	207	70
2 - 3	3.30	0.141	47.1	44	30
2 - 4	0.27	0.119	100.5	207	35
4 - 5	0.78	0.126	66.0	108	30
4 - 6	1.21	0.132	72.3	82	105
6 - 7	1.21	0.132	72.3	82	30
4 - 8	0.55	0.126	81.7	135	70
8 - 9	0.27	0.119	100.5	207	30
8 - 10	1.21	0.132	72.3	82	105
10 - 11	3.30	0.141	47.1	44	30
10 - 12	1.21	0.132	72.3	82	35
12 - 13	1.21	0.132	72.3	82	30
7 - 14	0.78	0.126	66.0	108	38
9 - 15	0.55	0.122	81.7	135	114.5
13 - 16	0.55	0.122	81.7	135	114.5
11 - 17	0.55	0.122	81.7	135	114.5
7 - 18	0.55	0.122	81.7	135	114.5
19 - 23	0.075	0.089	91.7	45	250
20 - 24	0.075	0.089	91.7	45	500
21 - 25	0.075	0.089	91.7	45	1000
22 - 26	0.075	0.089	91.7	45	2000
23 - 26	0.075	0.089	91.7	45	250
24 - 25	0.075	0.089	91.7	45	500
25 - 23	0.075	0.089	91.7	45	1000

In the perturb-and-observe-based method, the ground truth is obtained using (41) where the setpoint of the EMTP-RV simulation are individually perturbed with $\Delta 400\,\mathrm{W}$, $\Delta Q = 400\,\mathrm{VAr}$ and $\Delta V = 4\,\mathrm{V}$. The Jacobian matrix is computed using the PF algorithm presented in Section III for the same boundary conditions as the EMTP-RV model.

The results of the numerical validation are presented in Figure 4 as the distribution of the error between the proposed analytical model and the numerical methods (perturbation-based and Jacobian-based). The error distributions of certain nodes in the AC network, DC network and IC are shown. The colored bars represent the 80% quantiles and the maximum error is indicated. The balanced case is shown in blue, and the case with the unbalanced loading conditions is shown in yellow.

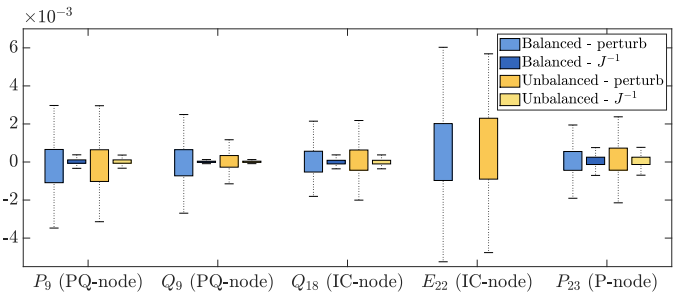

Fig. 4: 80% quantiles of the error of the proposed SC computation method for the hybrid 26-node microgrid. All values are in p.u.

It can be observed that the perturbation-based validation has a significantly larger error than the Jacobian-based validation. This is because a large perturbation value is needed due to the truncation error of the time-domain simulation. Because the SCs are more accurate in the region close to the

current operating point, the results are less accurate for larger perturbation values. Nonetheless, the analytical solution has an RMSE in the order of 10^{-4} p.u. and max error in the order of 10^{-3} p.u. Therefore, we can assert that the analytical method for the computation of the voltage SCs in hybrid AC/DC networks provides reliable estimates.

The computation of the voltage SCs takes on average $60\,\mathrm{ms}$ on a 2020 Apple Macbook Pro with an Intel Quad-Core i7 processor and 32 GB of RAM.

B. Multiterminal HVDC network

The proposed SC method is further validated on a large-scale transmission system that consists of two non-synchronous AC networks that are connected by two multiterminal HVDC grids. The networks topology, that has been originally proposed in [27], is given in Figure 5.

The two considered AC networks are the IEEE 57-bus and IEEE 14-bus reference systems. Both AC systems have a base voltage of $100\,\mathrm{kV}$ and a base power of $100\,\mathrm{MVA}$. The AC networks are interfaced using two separate HVDC networks of 7 nodes and 3 nodes, as shown in Figure 5. Both DC grids have a base voltage of $200\,\mathrm{kV}$ and a base power of $100\,\mathrm{MVA}$.

The proposed SC computational method is validated using the perturbation-based method where the PF of is recomputed after a small perturbation of 1×10^{-7} p.u. is applied. The perturbation is performed for every node individually. The results are summarised for each node type, i.e. PQ, PV, IC_{PQ}, $IC_{V_{dc}Q}$ and P_{dc} in Table IV. The RMSE and the maximum error are both in the order of 10^{-8}. Comparing these results to the validation for the 26-node hybrid microgrid, the error is significantly smaller. This is because the perturbation value is small and in the limit where the perturbation $\epsilon \to 0$, the numerical approximation in (41) becomes equal to the analytical closed from SC. The computation of the SC takes around $140\,\mathrm{ms}$.

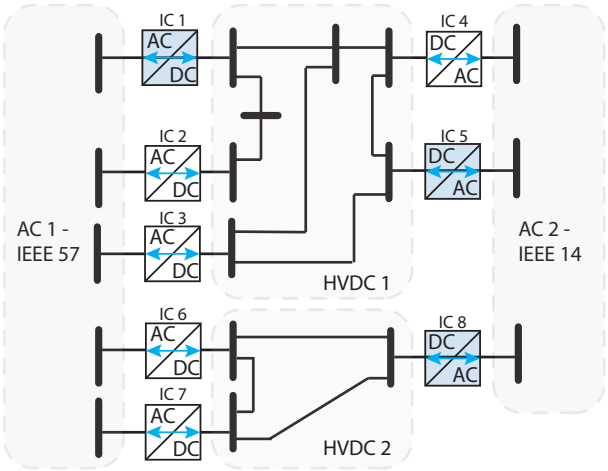

Fig. 5: Topology of the two multiterminal HVDC grids interfacing two non-synchronous AC grids. The interfacing converters in blue regulate the DC voltage

Node type	Network	RMSE [p.u.]	Max error [p.u.]
PQ	AC	1.72e-8	22.6e-8
PV	AC	1.85e-8	11.2e-8
P - Q	IC	1.45e-8	6.21e-8
V_{dc} - Q	IC	1.50e-8	6.22e-8
P_{dc}	DC	1.48e-8	5.44e-8

TABLE IV: The RMSE and maximum error of the proposed SC computation method for the multiterminal HVDC transmission network

VI. Conclusion

In this paper, we present a method for the analytical computation of the power flow SCs in balanced and unbalanced hybrid AC/DC networks. The SCs, defined as the partial derivatives of the nodal voltage with respect to the power injections, allow to formulate the grid constraints in the OPF problem in a fully linear way. Therefore, leveraging the real-time control of hybrid AC/DC networks. The proposed method is inspired by an existing SC computation process of solely AC networks and extended for hybrid networks using a unified PF model that accounts for the AC grid, DC grid and the various operation modes of the ICs. The uniqueness of the proposed SCs computational model is shown in a formal proof. The model is numerically validated on a 26-node hybrid AC/DC microgrid and on a multiterminal HVDC network that links two asynchronous AC transmission grids. It is shown that the accuracy of the SCs for the systems is in the order of 10^{-4} p.u. and 10^{-8} p.u., respectively. The computation time is around 10 to 100 ms and, therefore, within the limits for time-critical control applications.

Appendix A
Simplified Grid Example

To demonstrate the model, we will compute the sensitivity coefficients of a small hybrid example grid containing one PQ-node in the AC grid, one P-node in the DC grid, one interfacing converter and one AC slack node. The grid is shown in Figure 6. The line parameters and nodal voltage and power injections are given in Table V. The base values are the same as for the hybrid microgrid of Section V-A.

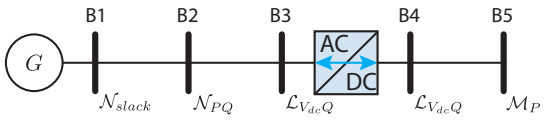

Fig. 6: Topology of the simplified example grid

Line	R (Ω)	X (Ω)	B (μS)
1 - 2	0.019	8.3e−3	7.1
2 - 3	0.1	4.2e−3	1.4
4 - 5	0.018	0.022	11.3

Bus	Nodal Voltage	Power inj.
1	1	$0.15 + 0.2i$
2	$0.997\angle 1.6\mathrm{e}{-3}$	$0.4 + 0.2i$
3	$0.963\angle 26\mathrm{e}{-3}$	$-0.52 - 0.4i$
4	1	0.52
5	0.968	−0.5

TABLE V: Line parameters, nodal voltages and power injections of the considered grid.

The SCs are computed using the system of equations composed by (13), (14), (16), (20), (21), (24), (26), (31),

$$\left[\begin{array}{cc|c|cc} \overline{F}_{2,2}^{\phi'}+\overline{H}_{2}^{\phi'} & \overline{F}_{2,2}^{\phi''}-\overline{H}_{2}^{\phi''} & 0 & \overline{F}_{2,3}^{\phi'} & \overline{F}_{2,3}^{\phi''} \\ \overline{F}_{2,2}^{\phi''}+\overline{H}_{2}^{\phi''} & -\overline{F}_{2,2}^{\phi'}+\overline{H}_{2}^{\phi'} & 0 & \overline{F}_{2,3}^{\phi'} & -\overline{F}_{2,3}^{\phi''} \\ \hline 0 & 0 & F_{5,5}+H_5 & 0 & 0 \\ \hline \overline{F}_{3,2}^{\phi'} & \overline{F}_{3,2}^{\phi''} & -F_{(4,5)} & \overline{F}_{3,3}^{\phi'}+\overline{H}_{3}^{\phi'} & \overline{F}_{3,3}^{\phi''}-\overline{H}_{3}^{\phi''} \\ \overline{F}_{3,2}^{\phi'} & -\overline{F}_{2,3}^{\phi''} & 0 & \overline{F}_{3,3}^{\phi''}+\overline{H}_{3}^{\phi''} & -\overline{F}_{3,3}^{\phi'}+\overline{H}_{3}^{\phi'} \end{array}\right] \left[\begin{array}{c} \partial\overline{E}_{2}^{\phi'}/\partial x \\ \partial\overline{E}_{2}^{\phi''}/\partial x \\ \partial E_5/\partial x \\ \partial\overline{E}_{3}^{\phi'}/\partial x \\ \partial\overline{E}_{3}^{\phi''}/\partial x \end{array}\right] = \left[\begin{array}{c} 1 \\ 0 \\ 0 \\ 0 \\ 0 \end{array}\right]_{x=P_2}, \left[\begin{array}{c} 0 \\ -1 \\ 0 \\ 0 \\ 0 \end{array}\right]_{x=Q_2}, \left[\begin{array}{c} 0 \\ 0 \\ -F_{5,4} \\ F_{4,4}+H_4 \\ 0 \end{array}\right]_{x=P_5}, \left[\begin{array}{c} 0 \\ 0 \\ 0 \\ 0 \\ -1 \end{array}\right]_{x=E_4}, \left[\begin{array}{c} 0 \\ 0 \\ 0 \\ 1 \\ 0 \\ 0 \end{array}\right]_{x=Q_3} \tag{42}$$

(33), (34) and (35). The system of equations of the 5-node hybrid grid is given in (V). The structure of $\mathbf{A}$ matrix and the $\mathbf{b}(x)$ vector is described in (36) and (37). The vector $b(x)$ is dependent on the controllable variable x, while the matrix A is constant. The variables F and H are straight-forward computed using the systems admittance matrix and the grids state as reported in (12). The SCs are analytically computed by solving this system of equations for every value of x.

The sensitivity matrices with respect to the active power (K_P), the reactive power (K_Q) and nodal voltages (K_V) are given in (43). The physical meaning of these sensitivity matrices is that if, e.g. the active power in node 2 increases by ΔP, the voltage in node 2 will increase by $(0.0120+0.0052i)\cdot\Delta P$ p.u. and in node 3 by $(0.0123+0.0048i)\cdot\Delta P$ p.u. The voltage of the other nodes remains unchanged as these are voltage-regulated nodes.

$$K_P = \begin{bmatrix} 0 & 0 & 0 & 0 & 0 \\ 0 & 0.0120+0.0052i & 0 & 0 & 0.0137+0.0060i \\ 0 & 0.0123+0.0048i & 0 & 0 & 0.0853+0.0084i \\ 0 & 0 & 0 & 0 & 0 \\ 0 & 0 & 0 & 0 & 0.069 \end{bmatrix},$$

$$K_Q = \begin{bmatrix} 0 & 0 & 0 & 0 & 0 \\ 0 & 0.0053-0.0119i & 0.0059-0.0116i & 0 & 0 \\ 0 & 0.0058-0.0116i & 0.0126-0.0734i & 0 & 0 \\ 0 & 0 & 0 & 0 & 0 \\ 0 & 0 & 0 & 0 & 0 \end{bmatrix},$$

$$K_V = \begin{bmatrix} 0 & 0 & 0 & 0 & 0 \\ 0 & 0 & 0 & 0.0005+0.0002i & 0 \\ 0 & 0 & 0 & 0.0028+0.0003i & 0 \\ 0 & 0 & 0 & 1 & 0 \\ 0 & 0 & 0 & 1.0345 & 0 \end{bmatrix} \tag{43}$$

These analytically computed SCs are compared with numerical ones that are obtained by perturbating the controllable variables. The magnitude of the perturbation is 1×10^{-7}. The results, represented as the RMSE and the maximum error between the analytically and the numerically computed voltage SCs, are shown in Table VI.

Ctrl. var.	**Network**	**RMSE** [p.u.]	**Max error** [p.u.]
P_2	*AC*	1.48e−8	3.18e−8
Q_2	*AC*	0.47e−8	0.75e−8
P_5	*IC*	0.41e−8	0.75e−8
E_4	*IC*	2.56e−8	4.53e−8
Q_3	*DC*	1.67e−8	3.47e−8

TABLE VI: The RMSE and maximum error of the analytical computed SC for the different node types for the simplified grid example

APPENDIX B
PROOF OF UNIQUENESS

The system of equations (13), (14), (16), (20), (21), (24), (26), (31), (33), (34) and (35) is linear with respect to the partial derivatives of the real and imaginary part of the nodal voltage. Therefore, the uniqueness of the solution, i.e. the voltage SCs, can be proved by showing that the homogeneous system of equations only has the trivial solution. The corollary is based on the main theorem in [23]. Because of space limitations, the proof is only shown for the system under balanced loading conditions.

Similarly to what has been done in [23], the linear system of equations given in Section IV can be written as in (44) where $\overline{\Delta}'$ and $\overline{\Delta}''$ are the unknown real and imaginary partial derivatives of the nodal voltages (in this case for both the AC and DC grids).

$$0 = \overline{H}_i^{\phi'}\overline{\Delta}_i' + \sum_{n\in\mathcal{N}}\overline{F}_{i,n}^{\phi'}\overline{\Delta}_n' - \overline{H}_i^{\phi''}\overline{\Delta}_i'' + \sum_{n\in\mathcal{N}}\overline{F}_{i,n}^{\phi''}\overline{\Delta}_n'' \qquad \forall i\in\mathcal{N}_{PQ}\cup\mathcal{N}_{PV} \tag{44a}$$

$$0 = \overline{H}_i^{\phi''}\overline{\Delta}_i' + \sum_{n\in\mathcal{N}}\overline{F}_{i,n}^{\phi'}\overline{\Delta}_n' + \overline{H}_i^{\phi'}\overline{\Delta}_i'' - \sum_{n\in\mathcal{N}}\overline{F}_{i,n}^{\phi''}\overline{\Delta}_n'' \qquad \forall i\in\mathcal{N}_{PQ} \tag{44b}$$

$$0 = \overline{E}_i^{\phi'}\overline{\Delta}_i' + \overline{E}_i^{\phi''}\overline{\Delta}_i'', \qquad \forall i\in\mathcal{N}_{PV} \tag{44c}$$

$$0 = H_j\overline{\Delta}_j + \sum_{m\in\mathcal{M}}F_{j,m}\Delta_m \qquad \forall j\in\mathcal{M}_P \tag{44d}$$

$$0 = \Delta_j, \qquad \forall j\in\mathcal{M}_V \tag{44e}$$

$$0 = H_k\Delta_k + \sum_{m\in\mathcal{M}}F_{k,m}\Delta_m \qquad \forall k\in\mathcal{L}_{PQ} \tag{44f}$$

$$0 = \overline{H}_i^{\phi'}\overline{\Delta}_l^{'} + \sum_{n\in\mathcal{N}}\overline{F}_{l,n}^{\phi'}\overline{\Delta}_n^{'} - \overline{H}_i^{\phi''}\overline{\Delta}_l^{''} + \sum_{n\in\mathcal{N}}\overline{F}_{l,n}^{\phi''}\overline{\Delta}_n^{''} \qquad \forall l\in\mathcal{L}_{PQ}, \tag{44g}$$

$$0 = \overline{H}_i^{\phi''}\overline{\Delta}_l^{'} + \sum_{n\in\mathcal{N}}\overline{F}_{l,n}^{\phi''}\overline{\Delta}_n^{'} + \overline{H}_i^{\phi'}\overline{\Delta}_l^{''} - \sum_{n\in\mathcal{N}}\overline{F}_{l,n}^{\phi'}\overline{\Delta}_n^{''} \qquad \forall l\in\mathcal{L}_{E_{dc}Q}\cup\mathcal{L}_{PQ} \tag{44h}$$

$$0 = \overline{H}_i^{\phi'}\overline{\Delta}_l^{'} + \sum_{n\in\mathcal{N}}\overline{F}_{l,n}^{\phi'}\overline{\Delta}_n^{'} - \overline{H}_i^{\phi''}\overline{\Delta}_l^{''} + \sum_{n\in\mathcal{N}}\overline{F}_{l,n}^{\phi''}\overline{\Delta}_n^{''} - \sum_{m\in\mathcal{M}\setminus\{k\}}F_{k,m}\Delta_m, \qquad \forall(l,k)\in\mathcal{L}_{E_{dc}Q} \tag{44i}$$

We want to show that the only solution to this system is the trivial one i.e., $\overline{\Delta}' = \overline{\Delta}'' = 0$. Let's consider two hybrid AC/DC networks with the same topology and the same parameters i.e., with identical $\overline{\mathbf{Y}}^{ac}$ and $\mathbf{Y}^{dc}$. The voltages in *network I* are given in (45) and the voltages in *network II* are given in (46) where ϵ is a positive real number.

$$\overline{E}_i^I = \overline{E}_i + \epsilon\overline{\Delta}_i, \qquad \forall i\in\mathcal{N}_{PQ}\cup\mathcal{N}_{PV} \tag{45a}$$

$$E_j^I = E_j + \epsilon\Delta_j, \qquad \forall j\in\mathcal{M}_P \tag{45b}$$

$$\overline{E}_l^1 = \overline{E}_l + \epsilon\overline{\Delta}_l, \qquad \forall l\in\mathcal{L}_{PQ}\cup\mathcal{L}_{V_{dc}Q} \tag{45c}$$

$$E_k^I = E_k + \epsilon\Delta_k, \qquad \forall k\in\mathcal{L}_{PQ} \tag{45d}$$

$$E_k^I = E_k, \qquad \forall k\in\mathcal{L}_{V_{dc}Q} \tag{45e}$$

$$E_j^I = E_j, \qquad \forall j\in\mathcal{M}_V \tag{45f}$$

$$\overline{E}_i^{II} = \overline{E}_i - \epsilon\overline{\Delta}_i, \qquad \forall i\in\mathcal{N}_{PQ}\cup\mathcal{N}_{PV} \tag{46a}$$

$$E_j^{II} = E_j - \epsilon\Delta_j, \qquad \forall j \in \mathcal{M}_P \tag{46b}$$
$$\overline{E}_l^{II} = \overline{E}_l - \epsilon\overline{\Delta}_l, \qquad \forall l \in \mathcal{L}_{PQ} \cup \mathcal{L}_{V_{dc}Q} \tag{46c}$$
$$E_k^{II} = E_k - \epsilon\Delta_k, \qquad \forall k \in \mathcal{L}_{PQ} \tag{46d}$$
$$E_k^{II} = E_k, \qquad \forall k \in \mathcal{L}_{V_{dc}Q} \tag{46e}$$
$$E_j^{II} = E_j, \qquad \forall j \in \mathcal{M}_V \tag{46f}$$

Using (1) we can formulate the PF equations for the two networks. We use the following notation for the complex AC voltages: $\overline{E}_i^I = \overline{E}_i^{I'} + j\overline{E}_i^{I''}$ and the identity F, defined in (12), is reformulated as $\overline{F}_{i,n}^{I,\phi} = \overline{F}_{i,n}^{\phi} + \epsilon\overline{F}_{i,n}^{\Delta,\phi}$, where $\overline{F}_{i,n}^{\Delta} = \Delta_i \underline{Y}_{i,n}^{ac}$. The PF equations of the first network are given in (47) and for the second network in (48). The equations are constructed starting from (1), the voltages (45) and (46) are substituted, and the equations are split into their real and imaginary part. Next, we subtract the PF models in (47) and (48) for network *I* and *II* to obtain (49).

$$P_i^{I,\phi} - P_i^{II,\phi} = \qquad \forall i \in \mathcal{N}_{PQ} \cup \mathcal{N}_{PV}$$
$$2\epsilon\Big(\overline{H}_i^{\phi'}\overline{\Delta}_i' + \sum_{n\in\mathcal{N}} \overline{F}_{i,n}^{\phi'}\overline{\Delta}_n' - \overline{H}_i^{\phi''}\overline{\Delta}_i'' + \sum_{n\in\mathcal{N}} \overline{F}_{i,n}^{\phi''}\overline{\Delta}_n''\Big) \tag{49a}$$
$$Q_i^{I,\phi} - Q_i^{II,\phi} = \qquad \forall i \in \mathcal{N}_{PQ}$$
$$2\epsilon\Big(\overline{H}_i^{\phi''}\overline{\Delta}_i' + \sum_{n\in\mathcal{N}} \overline{F}_{i,n}^{\phi'}\overline{\Delta}_n' + \overline{H}_i^{\phi'}\overline{\Delta}_i'' - \sum_{n\in\mathcal{N}} \overline{F}_{i,n}^{\phi''}\overline{\Delta}_n''\Big) \tag{49b}$$
$$|\overline{E}_i^{I\phi}|^2 - |\overline{E}_i^{II\phi}|^2 = 2\epsilon\Big(\overline{E}_i^{\phi'}\overline{\Delta}_i' + \overline{E}_i^{\phi''}\overline{\Delta}_i'',\Big), \forall i \in \mathcal{N}_{PV} \tag{49c}$$
$$P_j^I - P_j^{II} = 2\epsilon\Big(H_j\overline{\Delta}_j + \sum_{m\in\mathcal{M}} F_{j,m}\Delta_m\Big), \quad \forall j \in \mathcal{M}_P \tag{49d}$$
$$P_k^I - P_k^{II} = 2\epsilon\Big(H_k\Delta_k + \sum_{m\in\mathcal{M}} F_{k,m}\Delta_m\Big), \quad \forall k \in \mathcal{L}_{PQ} \tag{49e}$$
$$P_l^{I,\phi} - P_l^{II,\phi} = \qquad \forall l \in \mathcal{L}_{PQ}$$
$$2\epsilon\Big(\overline{H}_i^{\phi'}\overline{\Delta}_l^{'} + \sum_{n\in\mathcal{N}} \overline{F}_{l,n}^{\phi'}\overline{\Delta}_n^{'} - \overline{H}_i^{\phi''}\overline{\Delta}_l^{''} + \sum_{n\in\mathcal{N}} \overline{F}_{l,n}^{\phi''}\overline{\Delta}_n^{''}\Big) \tag{49f}$$
$$Q_l^{I,\phi} - Q_l^{II,\phi} = \qquad \forall l \in \mathcal{L}_{E_{dc}Q} \cup \mathcal{L}_{PQ}$$
$$2\epsilon\Big(\overline{H}_i^{\phi''}\overline{\Delta}_l^{'} + \sum_{n\in\mathcal{N}} \overline{F}_{l,n}^{\phi''}\overline{\Delta}_n^{'} + \overline{H}_i^{\phi'}\overline{\Delta}_l^{''} - \sum_{n\in\mathcal{N}} \overline{F}_{l,n}^{\phi'}\overline{\Delta}_n^{''}\Big) \tag{49g}$$
$$(47h) - (48h) = \qquad \forall (l,k) \in \mathcal{L}_{E_{dc}Q}$$
$$2\epsilon\Big(\overline{H}_i^{\phi'}\overline{\Delta}_l^{'} + \sum_{n\in\mathcal{N}} \overline{F}_{l,n}^{\phi'}\overline{\Delta}_n^{'} - \overline{H}_i^{\phi''}\overline{\Delta}_l^{''} + \sum_{n\in\mathcal{N}} \overline{F}_{l,n}^{\phi''}\overline{\Delta}_n^{''}$$
$$- \sum_{m\in\mathcal{M}\setminus\{k\}} F_{k,m}\Delta_m\Big) \tag{49h}$$

By substituting (44) into (49), it follows that:

$$\begin{aligned}
&P_i^{I,\phi} = P_i^{II,\phi} && \forall i \in \mathcal{N}_{PQ} \cup \mathcal{N}_{PV},\\
&Q_i^{I,\phi} = Q_i^{II,\phi} && \forall i \in \mathcal{N}_{PQ},\\
&P_j^I = P_j^{II} && \forall j \in \mathcal{M}_P,\\
&P_k^I = P_k^{II} && \forall k \in \mathcal{L}_{PQ},\\
&P_l^{I,\phi} = P_l^{II,\phi} && \forall l \in \mathcal{L}_{PQ},\\
&Q_l^{I,\phi} = Q_l^{II,\phi} && \forall l \in \mathcal{L}_{PQ} \cup \mathcal{L}_{V_{dc}Q}\\
&|\overline{E}_i^{I\phi}| = |\overline{E}_i^{II\phi}| && \forall i \in \mathcal{N}_{PV},\\
&E_j^I = E_j^{II} && \forall j \in \mathcal{M}_V,\\
&E_k^I = E_k^{II} && \forall k \in \mathcal{L}_{V_{dc}Q}.
\end{aligned} \tag{50}$$

Therefore, network *I* and *II* have the same power injections in the power-controllable nodes and the same voltages at the voltage-controllable nodes. According to the hypothesis in **Corollary 1**, the PF Jacobian, i.e. the derivative of the unified PF equations, is invertible. Next, we apply the inverse function theorem that states that the PF equations are also invertible in a neighbourhood around the current operating point. Assume we take an ϵ arbitrary small so all the voltages $\overline{E}^I$ and $\overline{E}^{II}$ belong to this neighbourhood with a one-to-one mapping between the voltages and the power injections. Because we showed before in (49) that the active and reactive power injections are exactly the same in network *I* and network *II*, the voltages $\overline{E}^I$ and $\overline{E}^{II}$ must also be exactly the same. Therefore, (45) = (46), and thus $\overline{\Delta}_i, \Delta_j, \overline{\Delta}_l, \Delta_k = 0$ for all $i \in \mathcal{N}, j \in \mathcal{M}, (l,k) \in \mathcal{L}$. Therefore, the homogeneous system of equations in (44) only has the trivial solution and the uniqueness of the solution is proved.

REFERENCES

[1] N. Eghtedarpour and E. Farjah, "Power control and management in a hybrid ac/dc microgrid," *IEEE transactions on smart grid*, vol. 5, no. 3, pp. 1494–1505, 2014.

[2] Y. R. Li, F. Nejabatkhah, and H. Tian, *Smart Hybrid AC/DC Microgrids*. Wiley-IEEE Press, 2023, pp. 1–20.

[3] D. K. Molzahn, F. Dörfler, H. Sandberg, S. H. Low, S. Chakrabarti, R. Baldick, and J. Lavaei, "A survey of distributed optimization and control algorithms for electric power systems," *IEEE Transactions on Smart Grid*, vol. 8, no. 6, pp. 2941–2962, 2017.

[4] T. Wu, C. Zhao, and Y. J. Zhang, "Distributed ac-dc optimal power dispatch of vsc-based energy routers in smart microgrids," *IEEE Transactions on Power Systems*, 2021.

[5] S. Bahrami, F. Therrien, V. W. Wong, and J. Jatskevich, "Semidefinite relaxation of optimal power flow for ac–dc grids," *IEEE Transactions on Power Systems*, vol. 32, no. 1, pp. 289–304, 2016.

[6] J. Renedo, A. A. Ibrahim, B. Kazemtabrizi, A. Garcia-Cerrada, L. Rouco, Q. Zhao, and J. Garcia-Gonzalez, "A simplified algorithm to solve optimal power flows in hybrid vsc-based ac/dc systems," *International Journal of Electrical Power & Energy Systems*, vol. 110, pp. 781–794, 2019.

[7] A. Alvarez-Bustos, B. Kazemtabrizi, M. Shahbazi, and E. Acha-Daza, "Universal branch model for the solution of optimal power flows in hybrid ac/dc grids," *International Journal of Electrical Power & Energy Systems*, vol. 126, p. 106543, 2021.

[8] R. D. Zimmerman, C. E. Murillo-Sánchez, and R. J. Thomas, "Matpower: Steady-state operations, planning, and analysis tools for power systems research and education," *IEEE Transactions on power systems*, vol. 26, no. 1, pp. 12–19, 2011.

[9] Q. Zhou and J. Bialek, "Simplified calculation of voltage and loss sensitivity factors in distribution networks," in *Proc. 16th Power Syst. Comput. Conf.(PSCC2008)*, 2008.

[10] T. R. Mendonca, M. E. Collins, M. F. Pinto, and T. C. Green, "Decentralisation of power flow solution for facilitating active network management," *CIRED-Open Access Proceedings Journal*, vol. 2017, no. 1, pp. 1669–1672, 2017.

[11] R. A. Jabr, "High-order approximate power flow solutions and circular arithmetic applications," *IEEE Transactions on Power Systems*, vol. 34, no. 6, pp. 5053–5062, 2019.

[12] S. Bolognani and S. Zampieri, "On the existence and linear approximation of the power flow solution in power distribution networks," *IEEE Transactions on Power Systems*, vol. 31, no. 1, pp. 163–172, 2015.

[13] A. Bernstein, C. Wang, E. Dall'Anese, J.-Y. Le Boudec, and C. Zhao, "Load flow in multiphase distribution networks: Existence, uniqueness, non-singularity and linear models," *IEEE Transactions on Power Systems*, vol. 33, no. 6, pp. 5832–5843, 2018.

[14] A. Bernstein and E. Dall'Anese, "Linear power-flow models in multiphase distribution networks," in *2017 IEEE PES Innovative Smart Grid Technologies Conference Europe (ISGT-Europe)*. IEEE, 2017, pp. 1–6.

[15] Z. Yang, H. Zhong, A. Bose, Q. Xia, and C. Kang, "Optimal power flow in ac–dc grids with discrete control devices," *IEEE Transactions on Power Systems*, vol. 33, no. 2, pp. 1461–1472, 2017.

[16] K. Christakou, J.-Y. LeBoudec, M. Paolone, and D.-C. Tomozei, "Efficient computation of sensitivity coefficients of node voltages and line currents in unbalanced radial electrical distribution networks," *IEEE Transactions on Smart Grid*, vol. 4, no. 2, pp. 741–750, 2013.

[17] K. Christakou, "Real-time optimal controls for active distribution networks: from concepts to applications," *European Journal of Organic Chemistry*, vol. 2012, pp. 7112–7119, 2015.

$$P_i^{I,\phi} = \overline{E}_i^{\phi'}\overline{H}_i^{\phi'} + \epsilon\sum_{n\in\mathcal{N}}\overline{F}_{i,n}^{\phi'}\underline{\Delta}_n^{'} + \epsilon\overline{\Delta}_i^{\phi'}\overline{H}_i^{\phi'} + \epsilon^2\sum_{n\in\mathcal{N}}\overline{F}_{i,n}^{\Delta\phi'}\underline{\Delta}_n^{'} - \overline{E}_i^{\phi''}\overline{H}_i^{\phi''} - \epsilon\sum_{n\in\mathcal{N}}\overline{F}_{i,n}^{\phi''}\underline{\Delta}_n^{''} - \epsilon\overline{E}_i^{\phi''}\overline{H}_i^{\phi''} - \epsilon^2\sum_{n\in\mathcal{N}}\overline{F}_{i,n}^{\Delta\phi''}\underline{\Delta}_n^{''}$$
$$\forall i \in \mathcal{N}_{PQ}\cup\mathcal{N}_{PV} \quad (47a)$$

$$Q_i^{I,\phi} = \overline{E}_i^{\phi'}\overline{H}_i^{\phi''} + \epsilon\sum_{n\in\mathcal{N}}\overline{F}_{i,n}^{\phi'}\underline{\Delta}_n^{''} + \epsilon\overline{\Delta}_i^{\phi'}\overline{H}_i^{\phi''} + \epsilon^2\sum_{n\in\mathcal{N}}\overline{F}_{i,n}^{\Delta\phi'}\underline{\Delta}_n^{''} + \overline{E}_i^{\phi''}\overline{H}_i^{\phi'} + \epsilon\sum_{n\in\mathcal{N}}\overline{F}_{i,n}^{\phi''}\underline{\Delta}_n^{'} + \epsilon\overline{E}_i^{\phi''}\overline{H}_i^{\phi'} + \epsilon^2\sum_{n\in\mathcal{N}}\overline{F}_{i,n}^{\Delta\phi''}\underline{\Delta}_n^{'}$$
$$\forall i \in \mathcal{N}_{PQ} \quad (47b)$$

$$|\overline{E}_i^{I\phi}|^2 = (\overline{E}_i^{\phi'})^2 + 2\epsilon\overline{E}_i^{\phi'}\overline{\Delta}_i^{'} + \epsilon^2(\overline{\Delta}_i^{'})^2 + (\overline{E}_i^{\phi''})^2 + 2\epsilon\overline{E}_i^{\phi''}\overline{\Delta}_i^{''} + \epsilon^2(\overline{\Delta}_i^{''})^2 \quad \forall i \in \mathcal{N}_{PV} \quad (47c)$$

$$P_j^I = E_jH_j + \epsilon\sum_{m\in\mathcal{M}}F_{j,m}\Delta_m + \epsilon\Delta_jH_j + \epsilon^2\sum_{m\in\mathcal{M}}F_{j,m}^{\Delta}\Delta_m \quad \forall j \in \mathcal{M}_P, \quad (47d)$$

$$P_k^I = E_kH_k + \epsilon\sum_{m\in\mathcal{M}}F_{k,m}\Delta_m + \epsilon\Delta_kH_k + \epsilon^2\sum_{m\in\mathcal{M}}F_{k,m}^{\Delta}\Delta_m \quad \forall k \in \mathcal{L}_{E_{dc}Q} \quad (47e)$$

$$P_l^{I,\phi} = \overline{E}_l\phi'\overline{H}_l^{\phi'} + \epsilon\sum_{n\in\mathcal{N}}\overline{F}_{l,n}^{\phi'}\underline{\Delta}_n^{'} + \epsilon\overline{\Delta}_l^{\phi'}\overline{H}_l^{\phi'} + \epsilon^2\sum_{n\in\mathcal{N}}\overline{F}_{l,n}^{\Delta\phi'}\underline{\Delta}_n^{'} - \overline{E}_l^{\phi''}\overline{H}_l^{\phi''} - \epsilon\sum_{n\in\mathcal{N}}\overline{F}_{l,n}^{\phi''}\underline{\Delta}_n^{''} - \epsilon\overline{E}_l^{\phi''}\overline{H}_l^{\phi''} - \epsilon^2\sum_{n\in\mathcal{N}}\overline{F}_{l,n}^{\Delta\phi''}\underline{\Delta}_n^{''}$$
$$\forall l \in \mathcal{L}_{PQ}, \quad (47f)$$

$$Q_l^{I,\phi} = \overline{E}_l^{\phi'}\overline{H}_l^{\phi''} + \epsilon\sum_{n\in\mathcal{N}}\overline{F}_{l,n}^{\phi'}\underline{\Delta}_n^{''} + \epsilon\overline{\Delta}_l^{\phi'}\overline{H}_l^{\phi''} + \epsilon^2\sum_{n\in\mathcal{N}}\overline{F}_{l,n}^{\Delta\phi'}\underline{\Delta}_n^{''} + \overline{E}_l^{\phi''}\overline{H}_l^{\phi'} + \epsilon\sum_{n\in\mathcal{N}}\overline{F}_{l,n}^{\phi''}\underline{\Delta}_n^{'} + \epsilon\overline{E}_l^{\phi''}\overline{H}_l^{\phi'} + \epsilon^2\sum_{n\in\mathcal{N}}\overline{F}_{l,n}^{\Delta\phi''}\underline{\Delta}_n^{'}$$
$$\forall l \in \mathcal{L}_{E_{dc}Q}\cup\mathcal{L}_{PQ} \quad (47g)$$

$$E_k^{I*}Y_{k,k}^{dc}E_k^{I*} + \sum_{m\in\mathcal{M}\setminus\{k\}}Y_{k,m}^{dc}E_m + \epsilon\sum_{m\in\mathcal{M}\setminus\{k\}}Y_{k,m}^{dc}\Delta_m = \quad \forall (l,k) \in \mathcal{L}_{E_{dc}Q}$$
$$\overline{E}_l\phi'\overline{H}_l^{\phi'} + \epsilon\sum_{n\in\mathcal{N}}\overline{F}_{l,n}^{\phi'}\underline{\Delta}_n^{'} + \epsilon\overline{\Delta}_l^{\phi'}\overline{H}_l^{\phi'} + \epsilon^2\sum_{n\in\mathcal{N}}\overline{F}_{l,n}^{\Delta\phi'}\underline{\Delta}_n^{'} - \overline{E}_l^{\phi''}\overline{H}_l^{\phi''} - \epsilon\sum_{n\in\mathcal{N}}\overline{F}_{l,n}^{\phi''}\underline{\Delta}_n^{''} - \epsilon\overline{E}_l^{\phi''}\overline{H}_l^{\phi''} - \epsilon^2\sum_{n\in\mathcal{N}}\overline{F}_{l,n}^{\Delta\phi''}\underline{\Delta}_n^{''} \quad (47h)$$

$$P_i^{II,\phi} = \overline{E}_i^{\phi'}\overline{H}_i^{\phi'} - \epsilon\sum_{n\in\mathcal{N}}\overline{F}_{i,n}^{\phi'}\underline{\Delta}_n^{'} - \epsilon\overline{\Delta}_i^{\phi'}\overline{H}_i^{\phi'} + \epsilon^2\sum_{n\in\mathcal{N}}\overline{F}_{i,n}^{\Delta\phi'}\underline{\Delta}_n^{'} - \overline{E}_i^{\phi''}\overline{H}_i^{\phi''} + \epsilon\sum_{n\in\mathcal{N}}\overline{F}_{i,n}^{\phi''}\underline{\Delta}_n^{''} + \epsilon\overline{E}_i^{\phi''}\overline{H}_i^{\phi''} - \epsilon^2\sum_{n\in\mathcal{N}}\overline{F}_{i,n}^{\Delta\phi''}\underline{\Delta}_n^{''}$$
$$\forall i \in \mathcal{N}_{PQ}\cup\mathcal{N}_{PV} \quad (48a)$$

$$Q_i^{II,\phi} = \overline{E}_i^{\phi'}\overline{H}_i^{\phi''} - \epsilon\sum_{n\in\mathcal{N}}\overline{F}_{i,n}^{\phi'}\underline{\Delta}_n^{''} - \epsilon\overline{\Delta}_i^{\phi'}\overline{H}_i^{\phi''} + \epsilon^2\sum_{n\in\mathcal{N}}\overline{F}_{i,n}^{\Delta\phi'}\underline{\Delta}_n^{''} + \overline{E}_i^{\phi''}\overline{H}_i^{\phi'} - \epsilon\sum_{n\in\mathcal{N}}\overline{F}_{i,n}^{\phi''}\underline{\Delta}_n^{'} - \epsilon\overline{E}_i^{\phi''}\overline{H}_i^{\phi'} + \epsilon^2\sum_{n\in\mathcal{N}}\overline{F}_{i,n}^{\Delta\phi''}\underline{\Delta}_n^{'}$$
$$\forall i \in \mathcal{N}_{PQ} \quad (48b)$$

$$|\overline{E}_i^{II\phi}|^2 = (\overline{E}_i^{\phi'})^2 - 2\epsilon\overline{E}_i^{\phi'}\overline{\Delta}_i^{'} + \epsilon^2(\overline{\Delta}_i^{'})^2 + (\overline{E}_i^{\phi''})^2 - 2\epsilon\overline{E}_i^{\phi''}\overline{\Delta}_i^{''} + \epsilon^2(\overline{\Delta}_i^{''})^2 \quad \forall i \in \mathcal{N}_{PV} \quad (48c)$$

$$P_j^{II} = E_jH_j - \epsilon\sum_{m\in\mathcal{M}}F_{j,m}\Delta_m - \epsilon\Delta_jH_j + \epsilon^2\sum_{m\in\mathcal{M}}F_{j,m}^{\Delta}\Delta_m \quad \forall j \in \mathcal{M}_P, \quad (48d)$$

$$P_k^{II} = E_kH_k - \epsilon\sum_{m\in\mathcal{M}}F_{k,m}\Delta_m - \epsilon\Delta_kH_k + \epsilon^2\sum_{m\in\mathcal{M}}F_{k,m}^{\Delta}\Delta_m \quad \forall k \in \mathcal{L}_{E_{dc}Q} \quad (48e)$$

$$P_l^{II,\phi} = \overline{E}_l\phi'\overline{H}_l^{\phi'} - \epsilon\sum_{n\in\mathcal{N}}\overline{F}_{l,n}^{\phi'}\underline{\Delta}_n^{'} - \epsilon\overline{\Delta}_l^{\phi'}\overline{H}_l^{\phi'} + \epsilon^2\sum_{n\in\mathcal{N}}\overline{F}_{l,n}^{\Delta\phi'}\underline{\Delta}_n^{'} + \overline{E}_l^{\phi''}\overline{H}_l^{\phi''} + \epsilon\sum_{n\in\mathcal{N}}\overline{F}_{l,n}^{\phi''}\underline{\Delta}_n^{''} + \epsilon\overline{E}_l^{\phi''}\overline{H}_l^{\phi''} - \epsilon^2\sum_{n\in\mathcal{N}}\overline{F}_{l,n}^{\Delta\phi''}\underline{\Delta}_n^{''}$$
$$\forall l \in \mathcal{L}_{PQ}, \quad (48f)$$

$$Q_l^{II,\phi} = \overline{E}_l^{\phi'}\overline{H}_l^{\phi''} - \epsilon\sum_{n\in\mathcal{N}}\overline{F}_{l,n}^{\phi'}\underline{\Delta}_n^{''} - \epsilon\overline{\Delta}_l^{\phi'}\overline{H}_l^{\phi''} + \epsilon^2\sum_{n\in\mathcal{N}}\overline{F}_{l,n}^{\Delta\phi'}\underline{\Delta}_n^{''} - \overline{E}_l^{\phi''}\overline{H}_l^{\phi'} - \epsilon\sum_{n\in\mathcal{N}}\overline{F}_{l,n}^{\phi''}\underline{\Delta}_n^{'} - \epsilon\overline{E}_l^{\phi''}\overline{H}_l^{\phi'} + \epsilon^2\sum_{n\in\mathcal{N}}\overline{F}_{l,n}^{\Delta\phi''}\underline{\Delta}_n^{'}$$
$$\forall l \in \mathcal{L}_{E_{dc}Q}\cup\mathcal{L}_{PQ} \quad (48g)$$

$$E_k^{II*}Y_{k,k}^{dc}E_k^{II*} + \sum_{m\in\mathcal{M}\setminus\{k\}}Y_{k,m}^{dc}E_m - \epsilon\sum_{m\in\mathcal{M}\setminus\{k\}}Y_{k,m}^{dc}\Delta_m = \quad \forall (l,k) \in \mathcal{L}_{E_{dc}Q}$$
$$\overline{E}_l\phi'\overline{H}_l^{\phi'} - \epsilon\sum_{n\in\mathcal{N}}\overline{F}_{l,n}^{\phi'}\underline{\Delta}_n^{'} - \epsilon\overline{\Delta}_l^{\phi'}\overline{H}_l^{\phi'} + \epsilon^2\sum_{n\in\mathcal{N}}\overline{F}_{l,n}^{\Delta\phi'}\underline{\Delta}_n^{'} + \overline{E}_l^{\phi''}\overline{H}_l^{\phi''} + \epsilon\sum_{n\in\mathcal{N}}\overline{F}_{l,n}^{\phi''}\underline{\Delta}_n^{''} + \epsilon\overline{E}_l^{\phi''}\overline{H}_l^{\phi''} - \epsilon^2\sum_{n\in\mathcal{N}}\overline{F}_{l,n}^{\Delta\phi''}\underline{\Delta}_n^{''} \quad (48h)$$

[18] S. Fahmy and M. Paolone, "Analytical computation of power grids' sensitivity coefficients with voltage-dependent injections," in *2021 IEEE Madrid PowerTech*, 2021, pp. 1–6.

[19] R. Gupta, F. Sossan, and M. Paolone, "Performance assessment of linearized opf-based distributed real-time predictive control," in *2019 IEEE Milan PowerTech*. IEEE, 2019, pp. 1–6.

[20] W. Lambrichts and M. Paolone, "General and unified model of the power flow problem in multiterminal ac/dc networks," *Accepted for publication in IEEE Transactions on Power Systems*, 2023, publisher: arXiv.

[21] R. P. Barcelos and D. Dujić, "Direct current transformer impact on the dc power distribution networks," *IEEE Transactions on Smart Grid*, vol. 13, no. 4, pp. 2547–2556, 2022.

[22] R. Teodorescu, M. Liserre, and P. Rodriguez, *Grid converters for photovoltaic and wind power systems*. John Wiley & Sons, 2011.

[23] M. Paolone, J.-Y. Le Boudec, K. Christakou, and D.-C. Tomozei, "Optimal voltage control processes in active distribution networks," The Institution of Engineering and Technology-IET, Tech. Rep., 2015.

[24] S. Barsali, K. Strunz, and Z. Styczynski, "Cigre' task force c6.04.02: Developing benchmark models for integrating distributed energy resources," in *2006 IEEE Power Engineering Society GM*, 2005.

[25] W. Lambrichts, J. Mace, and M. Paolone, "Experimental validation of a grid-aware optimal control of hybrid ac/dc microgrids," *submitted to 2024 Power Systems Computation Conference (PCSS) 2024*, 2023, publisher: arXiv.

[26] "EMTP," https://www.emtp.com/, accessed: 2021-12-15.

[27] R. Chai, B. Zhang, J. Dou, Z. Hao, and T. Zheng, "Unified power flow algorithm based on the nr method for hybrid ac/dc grids incorporating vscs," *IEEE Transactions on Power Systems*, vol. 31, no. 6, pp. 4310–4318, 2016.

Willem Lambrichts received the B.Sc. degree in electrical engineering from the Catholic University of Leuven, Belgium in 2018 and the M.Sc in energy engineering from the Catholic University of Leuven in 2020. Since 2020, he has been pursuing his PhD degree at the Distributed Electrical Systems Laboratory, EPFL, Switzerland. His research interests include state estimation and optimal grid-aware control in the domain of hybrid AC/DC distribution networks.

Mario Paolone (M'07, SM'10, F'22) received the M.Sc. (Hons.) and Ph.D. degrees in electrical engineering from the University of Bologna, Italy, in 1998 and 2002. In 2005, he was an Assistant Professor in power systems at the University of Bologna, where he was with the Power Systems Laboratory until 2011. Since 2011, he has been with the Swiss Federal Institute of Technology, Lausanne, Switzerland, where he is a Full Professor and the Chair of the Distributed Electrical Systems Laboratory. His research interests focus on power systems with particular reference to real-time monitoring and operational aspects, power system protections, dynamics and transients. Dr Paolone's most significant contributions are in the field of PMU-based situational awareness of Active Distribution Networks (ADNs) and in the field of exact, convex and computationally efficient methods for the optimal planning and operation of ADNs. Dr. Paolone was the founder and Editor-in-Chief of the Elsevier journal Sustainable Energy, Grids and Networks.